INTERACTION NOTES
Note 251
June 1975

ELECTROMAGNETIC EXCITATION OF A WIRE THROUGH AN APERTURE-PERFORATED, CONDUCTING SCREEN

by

Chalmers M. Butler

and

Korada R. Umashankar

Department of Electrical Engineering
University of Mississippi
University, Mississippi 38677

Abstract

Integro-differential equations are formulated for the general problem of a finite-length wire excited through an arbitrarily shaped aperture in a conducting screen. The wire is assumed to be electrically thin and perfectly conducting, and it is arbitrarily oriented behind the perfectly conducting screen of infinite extent. A known, specified incident field illuminates the perforated-screen/wire structure. The integro-differential equations fully account for the coupling between the wire and the aperture/screen. They are specialized to the case of the wire parallel to the screen with the aperture a narrow slot of general length. These special equations are solved numerically and data are presented for wire currents and aperture fields under selected conditions of wire/slot lengths and orientation. Data indicative of the coupling between the wire and slot are presented.

INTRODUCTION

The purpose of this paper is to present an analysis of the problem of a wire excited by an electromagnetic field which penetrates an aperture-perforated, conducting screen. General, coupled integro-differential equations are formulated in the paper with the wire current and aperture electric field (or equivalent aperture magnetic current) as unknowns. The coupling between the aperture and the wire is accounted for fully in the derived equations. These equations are specialized to the case in which the aperture is a narrow slot and the wire is parallel to the screen. Under these restricted but practical conditions, the appropriate equations are solved numerically and data are presented. Based upon the calculated results, the slot/wire problem is discussed in detail.

The general problem to be considered here is illustrated in Fig. 1 where one sees a finite-length wire which is arbitrarily oriented behind a planar conducting screen. The screen is assumed to be perfectly conducting, vanishingly thin, and of infinite extent. The wire is also perfectly conducting and is thin relative to its length as well as to the wavelength of the electromagnetic field. There is an aperture A of general shape in the screen of Fig. 1, and an incident field $(\bar{E}^i, \bar{H}^i)$ is seen impinging upon the structure. The wire is excited by the electromagnetic field which penetrates the aperture.

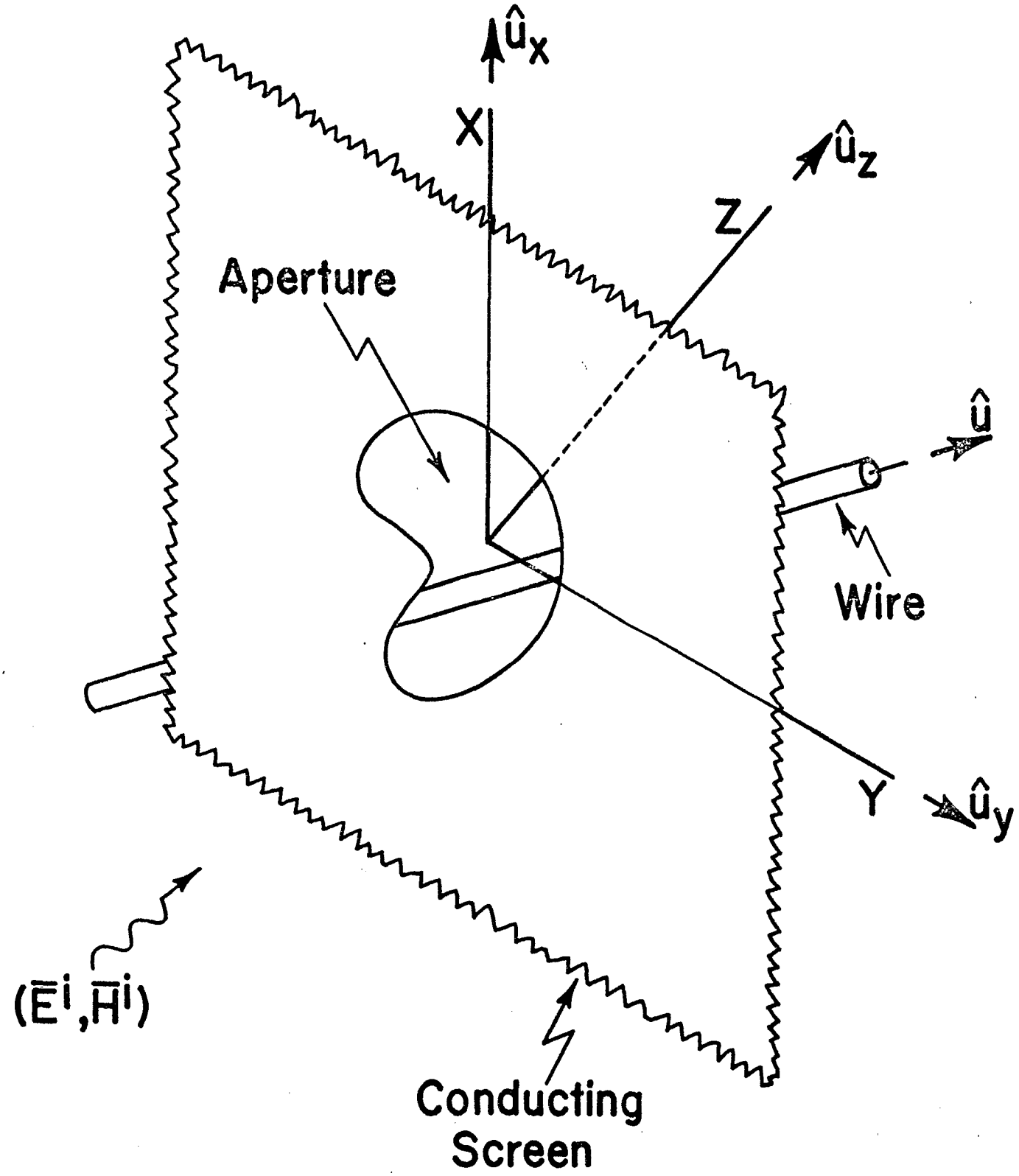

Fig. 1. Wire Illuminated through Aperture-Perforated Conducting Screen.

The only previous literature which has a bearing on the present work comprises one moderately related paper by King and Owyang [1], one by Lin, Curtis, and Vincent [2], and a preliminary version of the present work by Butler [3]. In the first paper above, the authors treat an array consisting of two driven dipoles symmetrically-located on either side of a slotted screen. Lin, Curtis, and Vincent consider a wire excited through an aperture but, since they calculate aperture fields in the absence of the wire, their theory does not include the complete coupling between the wire and aperture. As substantiated in the discussion below, the energy scattered back into the aperture by the wire, which is ignored by Lin, Curtis, and Vincent, can be quite significant and can strongly influence the aperture fields.

FORMULATION

In the boundary value problem under consideration here, one observes that there exists some total electric field $\bar{E}_t^A$ in the aperture A and tangential to the aperture/screen plane. This electric field is, of course, unknown <u>a priori</u> and, in fact, is the quantity which is to be determined as a solution to the problem. In terms of this aperture field $\bar{E}_t^A$, the incident field $(\bar{E}^i, \bar{H}^i)$, and the geometry of the structure, as depicted in Fig. 1, one can express the magnetic field in each half-space in such a way that Maxwell's equations are satisfied in each half-space and boundary conditions are satisfied on the screen

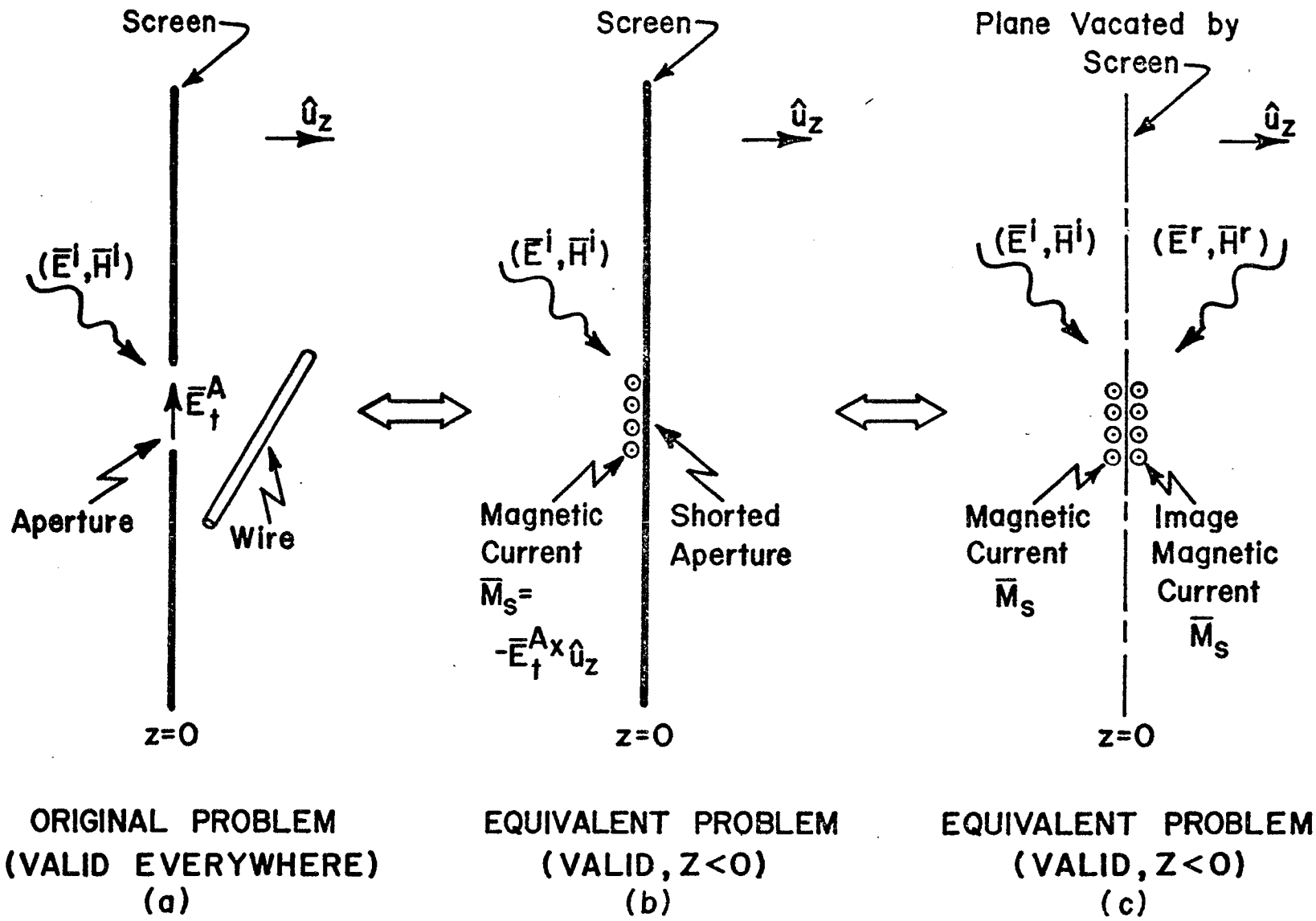

Fig. 2. Illuminated Half-Space Equivalences.

and on the wire. The magnetic field in each half-space is written as a function of $\bar{E}_t^A$, which is common to both half-spaces, ensuring continuity of electric field through A. Equating the transverse components of these two expressions for magnetic field enforces continuity of magnetic field through the aperture and leads directly to desired equations for the problem under investigation.

Fig. 2 depicts schematically* a step-by-step reduction of the left half-space ($z<0$) problem to a simple equivalent problem in a form which readily suggests how one may develop an expression for the left half-space total magnetic field $\bar{H}^-$. In Fig. 2a is seen the original problem while in Fig. 2b the aperture/screen is replaced by a perfectly conducting, continuous plane (aperture shorted) with the original tangential electric field $\bar{E}_t^A$ in the aperture restored at $z=0^-$, $(x,y)\varepsilon A$, by an appropriate magnetic surface current $\bar{M}_s$ which is specified to have a value $-\bar{E}_t^A \times \hat{u}_z$, i.e., $\bar{M}_s = -\bar{E}_t^A \times \hat{u}_z$. Notice that this as-of-yet undetermined magnetic current, which resides on the illuminated side of the shorted screen, radiates in the presence of the screen and that $(\bar{E}^i, \bar{H}^i)$ of the original problem in Fig. 2a illuminates the shorted screen. Next, in Fig. 2c, one appeals to image theory which enables him to remove the conducting screen entirely and which requires that he include the image magnetic current plus $(\bar{E}^r, \bar{H}^r)$, the field reflected

*Directions of vector quantities shown in Figs. 2 and 3 are adopted for illustrative purposes and are not intended to indicate properties of final results.

from the shorted screen, so that the total electromagnetic field in the left half-space is unchanged from its value in the original problem (Fig. 2a). These last modifications leading to Fig. 2c simply serve to preserve the boundary conditions on the xy-plane in the absence of the conducting screen, which are guaranteed by the presence of this screen in Fig. 2b. The equivalent problems illustrated in Figs. 2b and 2c are valid only in the left half-space so the fields $(\bar{E}^i,\bar{H}^i)$ and $(\bar{E}^r,\bar{H}^r)$, plus that radiated by the magnetic current and its image, are to be calculated only for $z<0$. Furthermore, since in the final equivalence of Fig. 2c all currents and fields exist in a homogeneous medium of infinite extent, one may use only the particular integral solutions of the wave equation for vector potential to calculate fields radiated by the magnetic current.

The total magnetic field $\bar{H}^-$ in the region $z<0$ of Fig. 2c is the sum of that radiated by $2\bar{M}_s$, the incident field $\bar{H}^i$, and $\bar{H}^r$. If one defines the so-called short-circuit field $(\bar{E}^{sc}, \bar{H}^{sc})$ to be the sum of the incidence and reflected fields, $\bar{E}^{sc}=\bar{E}^i+\bar{E}^r$ and $\bar{H}^{sc}=\bar{H}^i+\bar{H}^r$, in the half-space $z<0$ with the aperture shorted, he may construct the total magnetic field at a point $\bar{r}$ in the left half-space as

$$\bar{H}^-(\bar{r}) = \bar{H}^{sc}(\bar{r}) - j\frac{\omega}{k^2}\left[k^2\bar{F}(\bar{r}) + \text{grad}\left(\text{div } \bar{F}(\bar{r})\right)\right], \quad z<0 \quad . \quad (1)$$

In Eq. (1) ω is the angular frequency of the surpressed harmonic variation in time, $e^{j\omega t}$, k is 2π/wavelength λ and $\bar{F}$ is the

electric vector potential:

$$\bar{F}(\bar{r}) = \frac{\varepsilon}{4\pi} \iint_A 2\bar{M}_s(\bar{r}')G(\bar{r},\bar{r}')ds' \qquad (2)$$

where ε is the permittivity of the medium of Fig. 1 and where

$$G(\bar{r},\bar{r}') = \frac{e^{-jk|\bar{r}-\bar{r}'|}}{|\bar{r}-\bar{r}'|} \qquad (3)$$

with

$$|\bar{r}-\bar{r}'| = \left[(x-x')^2 + (y-y')^2 + z^2\right]^{\frac{1}{2}} , \quad (x',y')\varepsilon A , \quad z<0 \quad . \qquad (4)$$

Next, attention is turned to the equivalences illustrated in Fig. 3 and the formulation of equations peculiar to the right half-space (z>0). The unknown aperture electric field $\bar{E}_t^A$, common to the left and right half-space problems, is again postulated as illustrated in Fig. 3a. Fig. 3b depicts the conducting screen with the aperture short-circuited over which is impressed a surface magnetic current $-\bar{M}_s(=\bar{E}_t^A \times \hat{u}_z)$ that serves to maintain the original value of tangential electric field by supporting a discontinuity from zero at z=0 to $\bar{E}_t^A$ at $z=0^+$ in A. In the equivalent problem depicted in Fig. 3b, the wire remains, and both the wire current and the magnetic current radiate in the presence of the conducting screen. The final equivalence is the model shown in Fig. 3c from which the conducting screen

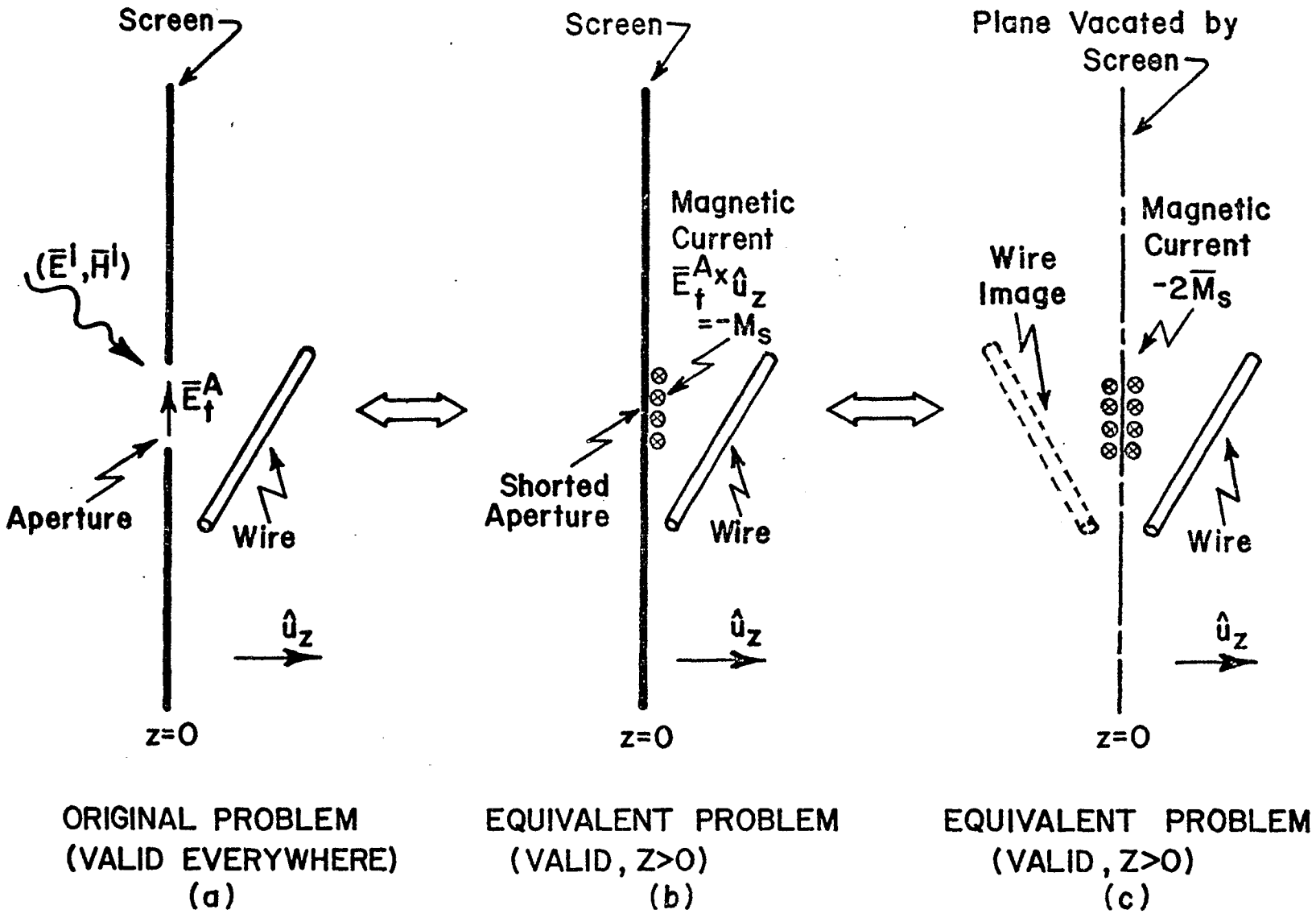

Fig. 3. Shadow Half-Space Equivalences.

has been removed. The boundary conditions on the electromagnetic field due to the presence of the conducting screen are maintained after the screen has been removed in Fig. 3c by the inclusion of the images of the wire and of the magnetic current. One may look upon the conducting wire's being replaced by an imaginary cylinder bearing an equivalent electric current, on whose surface one requires the total tangential electric field to be zero. For a wire satisfying the traditional assumptions of thin-wire theory, as is the case considered here, one neglects all but the axially directed surface current, which is assumed to be circumferentially independent, and accounts for it by a total axial current I. Furthermore, thin-wire assumptions permit one to require only that the axial component of electric field be zero on the wire surface. Subject to the qualifications above and the equivalence of Fig. 3c, one has achieved in the region $z>0$ a model having currents (both electric and magnetic) radiating in a homogeneous space of infinite extent. Again, such a situation permits one to employ only the particular integral solutions of the wave equations for the magnetic and electric vector potentials.

The total magnetic field in the region $z>0$ is denoted $\bar{H}^+$ and can be written

$$\bar{H}^+ = +j\frac{\omega}{k^2}\left[k^2\bar{F} + \text{grad}\left(\text{div } \bar{F}\right)\right] + \frac{1}{\mu}\,\text{curl } \bar{A}\ , \quad z>0\ , \qquad (5)$$

where $\bar{F}$ is defined in (2) and where μ is the permeability of the medium. $\bar{A}$ is the magnetic vector potential due to the wire

current plus its image:

$$\bar{A}(\bar{r}) = \frac{\mu}{4\pi}\,\hat{u}\int_L I(\bar{r}'_w)G(\bar{r},\bar{r}'_w)d\ell'$$

$$+\frac{\mu}{4\pi}\,\hat{u}_i\int_L I(\bar{r}'_i)G(\bar{r},\bar{r}'_i)d\ell' \quad , \qquad (6)$$

where $\hat{u}$ and $\hat{u}_i$ are unit vectors in the wire and wire image directions, respectively. The wire is of length L and radius a, and the vector $\bar{r}'_w$ locates a source point on the wire while $\bar{r}'_i$ locates a source point on the wire image.

As a part of the right half-space problem, one must enforce the appropriate boundary condition on the wire by requiring that the total electric field in the axial direction on the wire's surface be zero. To this end, one requires

$$\left[\bar{E}^A_w + \bar{E}^i_w + \bar{E}^s_w\right]\cdot\hat{u} = 0, \text{ on wire} \qquad (7)$$

where $\bar{E}^A_w$ is the field due to the aperture/screen, $\bar{E}^i_w$ is that due to the wire image, and $\bar{E}^s_w$ is that due to the equivalent sources on the wire. The terms in Eq. (7) can be written

$$\bar{E}^A_w = +\frac{1}{\varepsilon}\,\text{curl}\,\bar{F} \quad , \; z>0 \qquad (8)$$

$$\bar{E}^s_w + \bar{E}^i_w = -j\frac{\omega}{k^2}\left[k^2\bar{A} + \text{grad}\left(\text{div}\,\bar{A}\right)\right] \quad , \; z>0 \qquad (9)$$

so that (7) becomes

$$\frac{1}{\varepsilon}\,\hat{u}\cdot\operatorname{curl}\bar{F} \;-j\frac{\omega}{k^2}\,\hat{u}\cdot\left[\,k^2\bar{A} + \operatorname{grad}\left(\operatorname{div}\bar{A}\right)\right] = 0, \text{ on wire} \quad , \qquad (10)$$

an equation which demands that the wire boundary condition be honored.

One observes that the formulations of Eqs. (1), (5), and (10) are based on the magnetic and electric vector potentials, $\bar{A}$ and $\bar{F}$, which implies that $\bar{H}^+$ and $\bar{H}^-$ satisfy Maxwell's equations and the radiation condition in the appropriate half-spaces. Boundary conditions on the screen are satisfied because (1) and (5) are based upon the models of Figs. 2c and 3c, and Eq. (10) ensures that the tangential electric field along the wire surface be zero. $\bar{E}_t^A$ is common to both half-space formulations (through $\bar{M}_s$ and $\bar{F}$) so the final remaining condition that must be enforced is continuity of the total transverse magnetic field through the aperture, which serves to couple the two individual half-space formulations.

The continuity requirement on tangential magnetic field is

$$\lim_{z\uparrow 0}\ \bar{H}^- \times \hat{u}_z = \lim_{z\downarrow 0}\ \bar{H}^+ \times \hat{u}_z$$

which, in view of Eqs. (1) and (5), becomes

$$j2\frac{\omega}{k^2}\left[k^2\bar{F} + \text{grad}\left(\text{div } \bar{F}\right)\right]^{\times} \hat{u}_z + \frac{1}{\mu}\left(\text{curl } \bar{A}\right)^{\times} \hat{u}_z = \bar{H}^{sc\times} \hat{u}_z \quad , \quad (11)$$

$$\begin{cases} \text{in } A \\ z = 0 \end{cases} .$$

Since $\bar{H}^{sc\times} \hat{u}_z = 2\bar{H}^{i\times} \hat{u}_z$ at $z=0$ on the shorted screen, Eq. (11) reduces to

$$j\frac{\omega}{k^2}\left[k^2\bar{F} + \text{grad}\left(\text{div } \bar{F}\right)\right]^{\times} \hat{u}_z + \frac{1}{2\mu}\left(\text{curl } \bar{A}\right)^{\times} \hat{u}_z = \bar{H}^{i\times} \hat{u}_z \quad , \quad (12)$$

$$\begin{cases} \text{in } A \\ z = 0 \end{cases} ,$$

which can be written in scalar form,

$$\left(\frac{\partial^2}{\partial x^2} + k^2\right) F_x + \frac{\partial^2}{\partial x \partial y} F_y + j\frac{\omega\varepsilon}{2}\left(\frac{\partial}{\partial z} A_y - \frac{\partial}{\partial y} A_z\right) = -j\frac{k^2}{\omega} H_x^i \quad , \quad (13a)$$

$$z = 0 \quad , \quad (x,y)\varepsilon A,$$

$$\left(\frac{\partial^2}{\partial y^2} + k^2\right) F_y + \frac{\partial^2}{\partial y \partial x} F_x + j\frac{\omega\varepsilon}{2}\left(\frac{\partial}{\partial x} A_z - \frac{\partial}{\partial z} A_x\right) = -j\frac{k^2}{\omega} H_y^i \quad , \quad (13b)$$

$$z = 0 \quad , \quad (x,y)\varepsilon A,$$

where

$$j\frac{\omega\varepsilon}{2}\left(\frac{\partial}{\partial z}A_y - \frac{\partial}{\partial y}A_z\right)_{z=0}$$

$$= -j\frac{\omega\mu\varepsilon}{4\pi}\int_{s'=-L/2}^{L/2} I(s')\left[z_c\cos\beta + (y-y_c)\cos\gamma\right]\tilde{G}(x,y;s')ds' \qquad (14a)$$

and

$$j\frac{\omega\varepsilon}{2}\left(\frac{\partial}{\partial x}A_z - \frac{\partial}{\partial z}A_x\right)_{z=0}$$

$$= +j\frac{\omega\mu\varepsilon}{4\pi}\int_{s'=-L/2}^{L/2} I(s')\left[z_c\cos\alpha + (x-x_c)\cos\gamma\right]\tilde{G}(x,y;s')ds' \qquad (14b)$$

with

$$\tilde{G}(x,y;s') = -\left(j\frac{k}{d^2} + \frac{1}{d^3}\right) e^{-jkd} \qquad (15a)$$

and

$$d(x,y,s') = \left[[x - (x_c + s'\cos\alpha)]^2 + [y - (y_c + s'\cos\beta)]^2 + (z_c + s'\cos\gamma)^2\right]^{\frac{1}{2}}. \qquad (15b)$$

F_x and F_y are components of $\bar{F}$ defined in (2) and the geometric quantities of interest in (14) and (15) are listed below.

Center of wire:

$$(x_c, y_c, z_c)$$

Unit vector along wire with sense of I:

$$\hat{u} = \cos\alpha\ \hat{u}_x + \cos\beta\ \hat{u}_y + \cos\gamma\ \hat{u}_z$$

Direction cosines of wire:

$$\cos\alpha = \hat{u}\cdot\hat{u}_x$$

$$\cos\beta = \hat{u}\cdot\hat{u}_y$$

$$\cos\gamma = \hat{u}\cdot\hat{u}_z$$

Also, (10) can be written as a scalar equation which appears on the following page and in which

$$g(s,s') = \frac{e^{-jkR(s,s')}}{R(s,s')} \tag{17a}$$

with

$$R(s,s') = \left[4z_c^2 + 4z_c(s+s')\cos\gamma + 4ss'\cos^2\gamma + (s-s')^2\right]^{\frac{1}{2}}. \tag{17b}$$

$$\left(\frac{\partial^2}{\partial s^2} + k^2\right) \int_{s'=-L/2}^{L/2} I(s') \frac{e^{-jk[a^2 + (s-s')^2]^{\frac{1}{2}}}}{[a^2 + (s-s')^2]^{\frac{1}{2}}} ds' + k^2(2\cos^2\gamma - 1) \int_{s'=-L/2}^{L/2} I(s')g(s,s')ds'$$

$$- \frac{\partial}{\partial s} \int_{s'=-L/2}^{L/2} \frac{d}{ds'} I(s')g(s,s')ds' = -j4\pi\omega \left[\frac{\partial}{\partial z} F_x \cos\beta - \frac{\partial}{\partial z} F_y \cos\alpha\right.$$

$$\left. + \left(\frac{\partial}{\partial x} F_y - \frac{\partial}{\partial y} F_x\right) \cos\gamma \right] , \text{ on the wire.} \qquad (16)$$

Specialization of Aperture to Narrow Slot of Finite Length

Without the wire, Fig. 1 would depict the traditional, general aperture/screen problem, and (13) with terms involving components of $\bar{A}$ deleted would be the appropriate set of integro-differential equations. Recently, a few researchers [4,5] have undertaken to solve numerically various non-circular aperture problems and have found computer storage and run times to be very high; the problem under consideration here of a wire excited through a general aperture is even more demanding of storage and time. Therefore, in order to reduce the present problem to a feasible size computer-wise and yet to retain the fundamental features of practical interest totally accounting for the coupling between the wire and the aperture, we next specialize the aperture geometry to be an electrically narrow slot of width w and length ℓ. The slotted screen is shown in Fig. 4 with the wire of length L and radius a centered at (x_c, y_c, z_c) in the shadow half-space and having arbitrary direction specified by the unit vector $\hat{u}$.

Narrow-slot assumptions, similar in principle to those invoked in thin-wire theory, can be employed here to simplify the analysis. When the slot is very narrow relative to the wavelength and long compared to its width, the electric field in the slot is principally transverse to the longer slot dimension (transverse to x in Fig. 4) and has a known transverse variation. This transverse variation of electric field, or equivalent magnetic current, can be determined via electrostatics and is found to be simply (see Fig. 4)

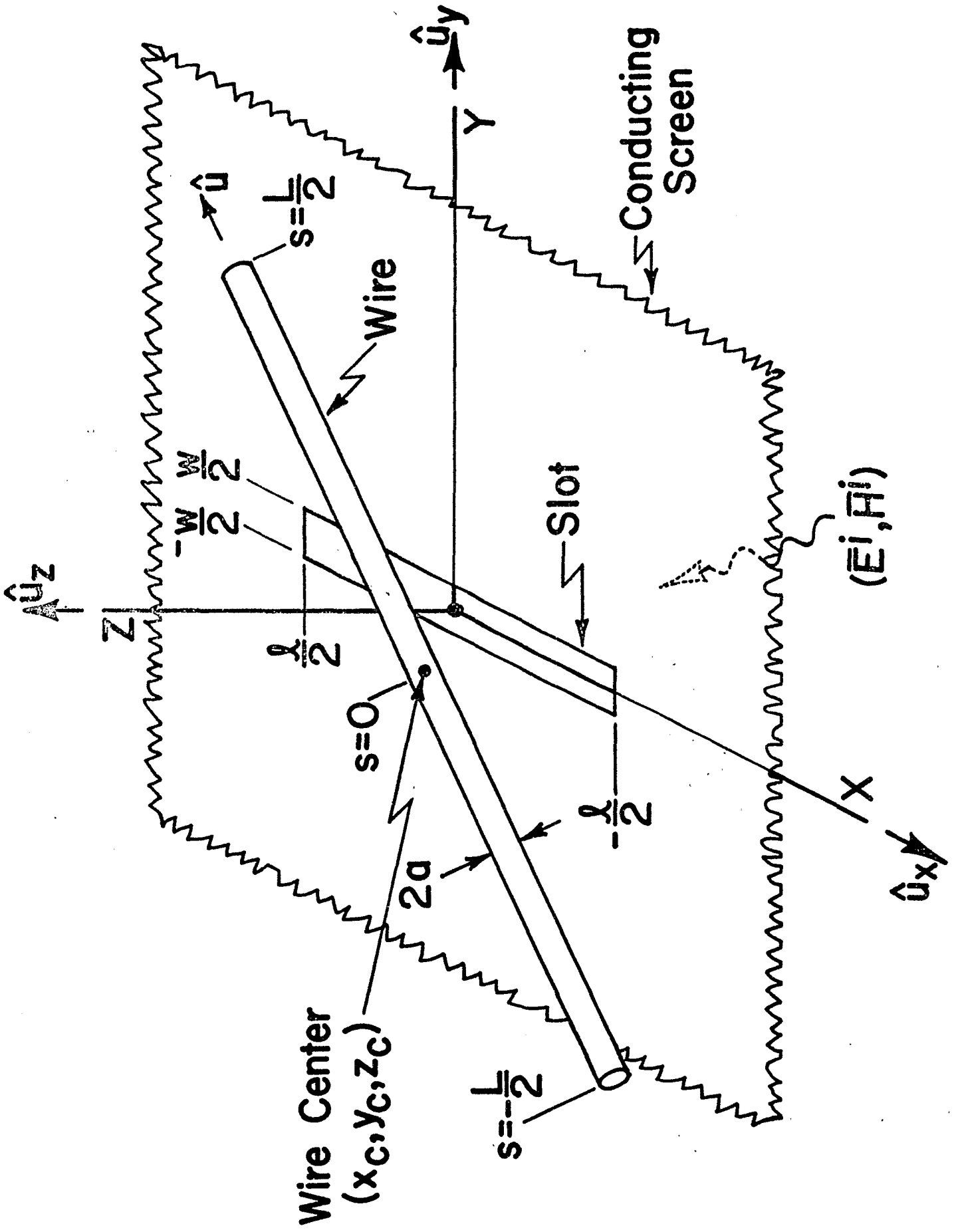

Fig. 4. Wire Illuminated through Slotted Screen.

$$\xi(y) = \frac{1/\pi}{\sqrt{\left(\frac{w}{2}\right)^2 - y^2}} \tag{18}$$

provided the slot excitation does not possess an appreciable component which is an odd function with respect to y. Ignoring the axial (x-component) electric field, or, transverse equivalent magnetic current, in the slot, which, of course, implies $F_y=0$, and evaluating quantities of interest along the slot axis (y=0,z=0), one reduces the surviving component of the electric vector potential F_x to

$$F_x(x,0,0) = \frac{\varepsilon}{2\pi}\int_{x'=-\ell/2}^{\ell/2} m(x') \int_{y'=-w/2}^{w/2} \xi(y') \frac{e^{-jk\left[(x-x')^2 + y'^2\right]^{\frac{1}{2}}}}{\left[(x-x')^2 + y'^2\right]^{\frac{1}{2}}} dy'dx' \tag{19}$$

where m(x) and $\xi(y)$ are the axial and transverse variations, respectively, of the slot magnetic current:

$$M_{s_x}(x,y) = m(x)\xi(y) . \tag{20}$$

Subject to the above expression for M_{s_x} and the integration variable transformation,

$$y' = \frac{w}{2} \sin\frac{\alpha}{2} ,$$

Eq. (19) becomes

$$F_x(x,0,0) = \frac{\epsilon}{2\pi}\int_{x'=-\ell/2}^{\ell/2} m(x')K(x-x';\tfrac{w}{4})dx' \qquad (21)$$

where the kernel is

$$K(\zeta,a) = \frac{1}{2\pi}\int_{\alpha=-\pi}^{\pi} \frac{e^{-jk[\zeta^2 + 4a^2\sin^2\frac{\alpha}{2}]^{\frac{1}{2}}}}{[\zeta^2 + 4a^2\sin^2\frac{\alpha}{2}]^{\frac{1}{2}}}\,d\alpha \quad , \qquad (22a)$$

$$\doteq \frac{e^{-jk[\zeta^2 + a^2]^{\frac{1}{2}}}}{[\zeta^2 + a^2]^{\frac{1}{2}}} \quad . \qquad (22b)$$

F_x of (21) with K of (22) is recognized to have the form of the magnetic vector potential associated with a thin wire of radius $\frac{w}{4}$. The same result relating the width to an equivalent radius may be obtained in a different way [6].

The above simplifications enable one to reduce Eqs. (13) to

$$\left(\frac{\partial^2}{\partial x^2} + k^2\right) F_x + j\frac{\omega\epsilon}{2}\left(\frac{\partial}{\partial z} A_y - \frac{\partial}{\partial y} A_z\right) = -j\frac{k^2}{\omega} H_x^i \quad . \qquad (23)$$

Eq. (16), with $F_y=0$, applies to the present case. Finally, under the further specialization that the wire be parallel to the screen, the particularly simple coupled integro-differential equations below are obtained:

$$\left(\frac{\partial^2}{\partial x^2} + k^2\right) \int_{x'=-\ell/2}^{\ell/2} m(x') K(x-x'; \tfrac{w}{4})\, dx' \quad + j\pi\omega \frac{\partial}{\partial z} A_y = -j2\pi\omega\mu\, H_x^i \quad , \quad \text{on slot} \tag{24a}$$

$$\left(\frac{\partial^2}{\partial s^2} + k^2\right) \int_{s'=-L/2}^{L/2} I(s') \left[K(s-s';a) - K(s-s';2z_c)\right] ds' \quad + j4\pi\omega \cos\beta \frac{\partial}{\partial z} F_x = 0 \quad , \quad \text{on wire.} \tag{24b}$$

RESULTS

Eqs. (24) have been solved numerically by the standard moment method [7] and selected results are presented below. In the following explanations of results, an effort is made to provide sufficient data to characterize the problem under study and, in particular, to outline how quantities of interest depend upon important geometric features of the slotted screen/wire problem. Also, the manner in which the incident field influences the electric currents on the wire and magnetic currents on the slot is mentioned.

In all cases for which results are given below, the wire is parallel to the screen and its center is designated (x_c, y_c, z_c). The slot center is at (0,0,0) and its longer dimension is along the x axis as shown in Fig. 4. In the following discussion of results, the angular rotation of the wire about its center is in a plane parallel to the screen and is measured by the angle β defined as the angular displacement from the y axis as illustrated in Fig. 5. When the narrow slot is viewed as the dual of a thin wire, subject to the usual thin-wire/narrow-slot assumptions, one readily sees that the wire is not excited by the fields which penetrate the slot whenever the two are parallel and, also, that the coupling between wire and slot is maximum when they are perpendicular.

It can be shown easily that, if the excitation of a thin wire or a narrow slot is an even function of axial displacement measured with respect to the center of the element, the current

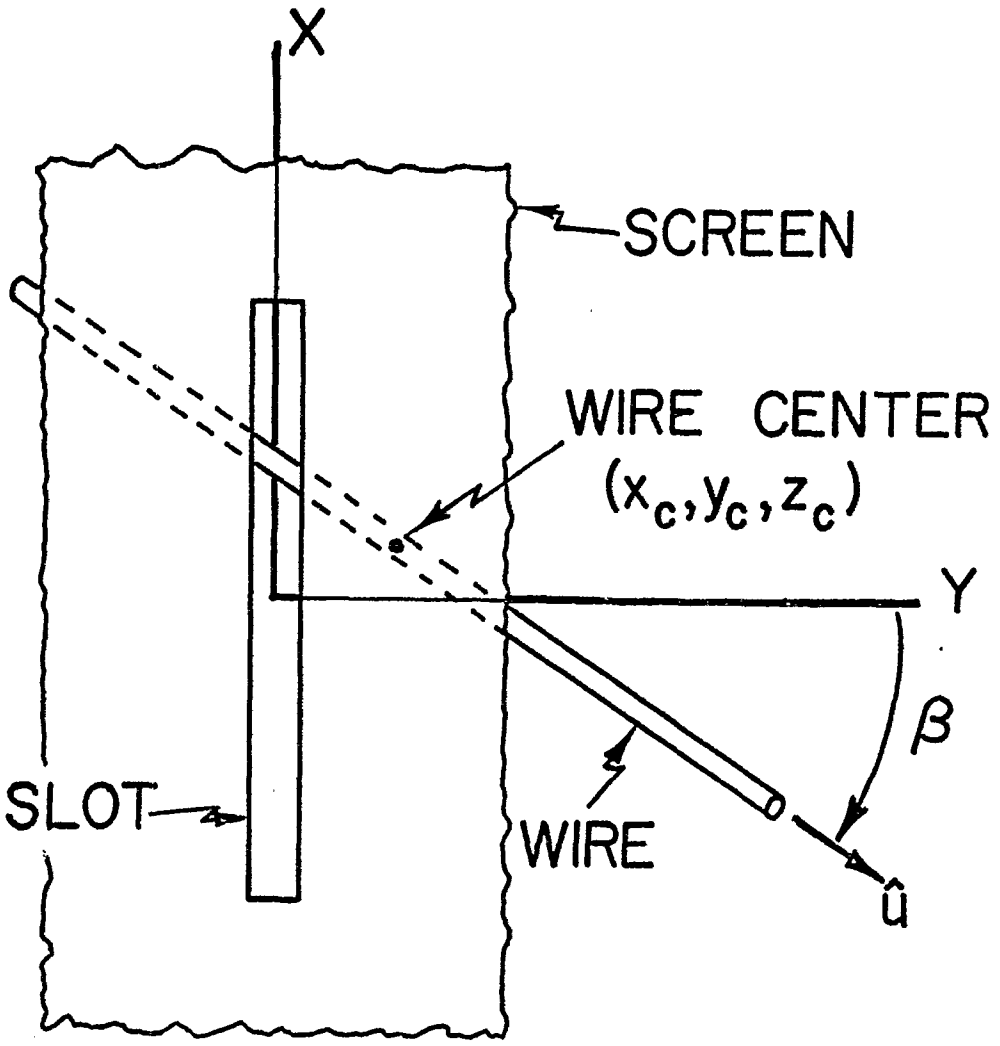

Fig. 5. Wire/Slot Orientation (Bottom View).

must be even too and, also, if the excitation is odd, so must be the current. In the case of a half-wavelength wire or slot, the resonant current is nearly cosinusoidal whereas, in a one-wavelength element, the antiresonant current is approximately a sine function. Hence, an odd-function excitation cannot excite a significant resonant component of current in a half-wavelength wire or slot, and an even-function excitation cannot excite an appreciable antiresonant component of current in a one-wavelength element. These observations, made relative to a wire in free space or a single slot in an infinite screen, also hold for a thin wire parallel to an infinite screen.

Half-Wavelength Slot, Half-Wavelength Wire

Fig. 6 shows the current I on a half-wavelength wire, as a function of position along the wire, induced by the field which penetrates a half-wavelength slot; this current is given for selected values of the angle β. When $\cos\beta=1$, the wire and slot are perpendicular, and the coupling is seen to be maximum as expected, while there is no coupling (hence the wire current is zero) when the wire and slot are parallel ($\cos\beta=0$). The wire current distribution is essentially a cosine function as one would expect for resonant length. As seen in Fig. 7 there is a small component of odd-function current on the resonant wire due to the asymmetric coupling to the slot caused by displacement of the wire center from the z axis. Also, since the wire is closer to the slotted screen in the case for which the data of the latter figure are given, the current is slightly

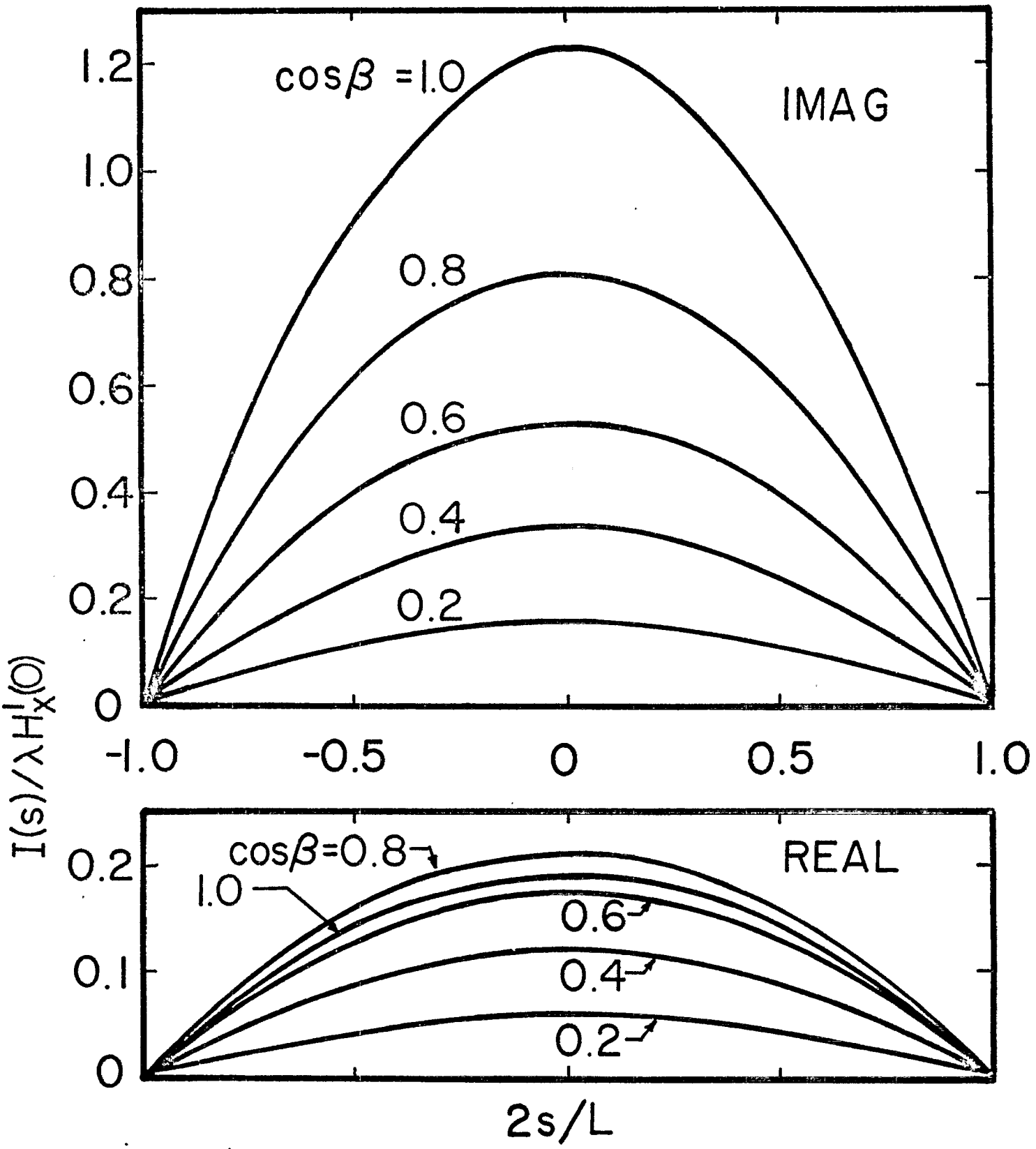

Fig. 6. Current on Wire Illuminated through Slotted Screen ($w/\lambda = 0.05$, $\ell/\lambda = 0.5$; $a/\lambda = 0.001$, $L/\lambda = 0.5$; $x_c/\lambda = 0$, $y_c/\lambda = 0$, $z_c/\lambda = 0.25$; normal incidence).

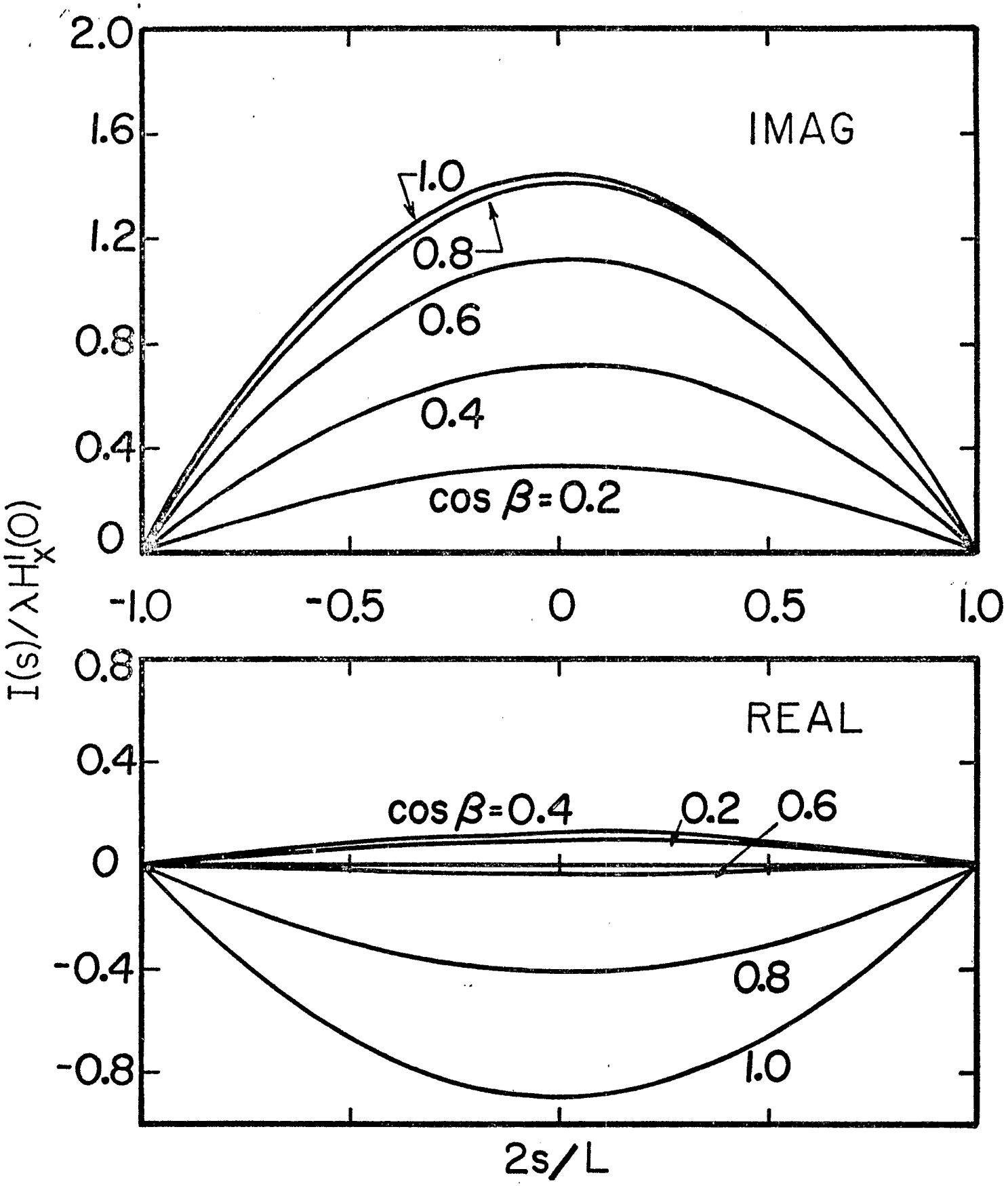

Fig. 7. Current on Wire Illuminated through Slotted Screen ($w/\lambda = 0.05$, $\ell/\lambda = 0.5$; $a/\lambda = 0.001$, $L/\lambda = 0.5$; $x_c/\lambda = 0.125$, $y_c/\lambda = 0$, $z_c/\lambda = 0.125$; normal incidence)

greater. With the wire center above the slot axis but not on the z axis, the illumination of the wire is always an even function with respect to its center whenever $\cos\beta=1$ but not for other angles. Hence, as seen in Fig. 7, I is strictly even only for $\cos\beta=1$; in Fig. 6, with the wire center on the z axis, the excitation of the wire is always even producing an even-function current. As pointed out subsequently, this effect is quite dramatic when the length of either the wire or the slot is one wavelength.

Figs. 8 and 9 depict the dependence of wire current on the location of the wire center.

In Fig. 10 is shown the axial distribution of magnetic current $m(x)$, or, equivalently, electric field, in the slot for several values of $\cos\beta$. Here we note that, when the wire and the slot are perpendicular ($\cos\beta=1$), the magnitude of the real part of the magnetic current is approximately twice that for the $\cos\beta=0$ case. The wire and slot are uncoupled when $\cos\beta=0$, and the curve so-designated represents the slot magnetic current in the absence of the wire. One readily appreciates from Fig. 10 how serious the errors may become in a two-step analyses in which, first, the slot field or magnetic current is calculated in the absence of the obstacle behind the screen and, second, induced current on the obstacle is calculated on the basis of illumination determined from the slot field of the first step. Not only does such a procedure lead to errors in magnitude but also to errors in phase (Fig. 10).

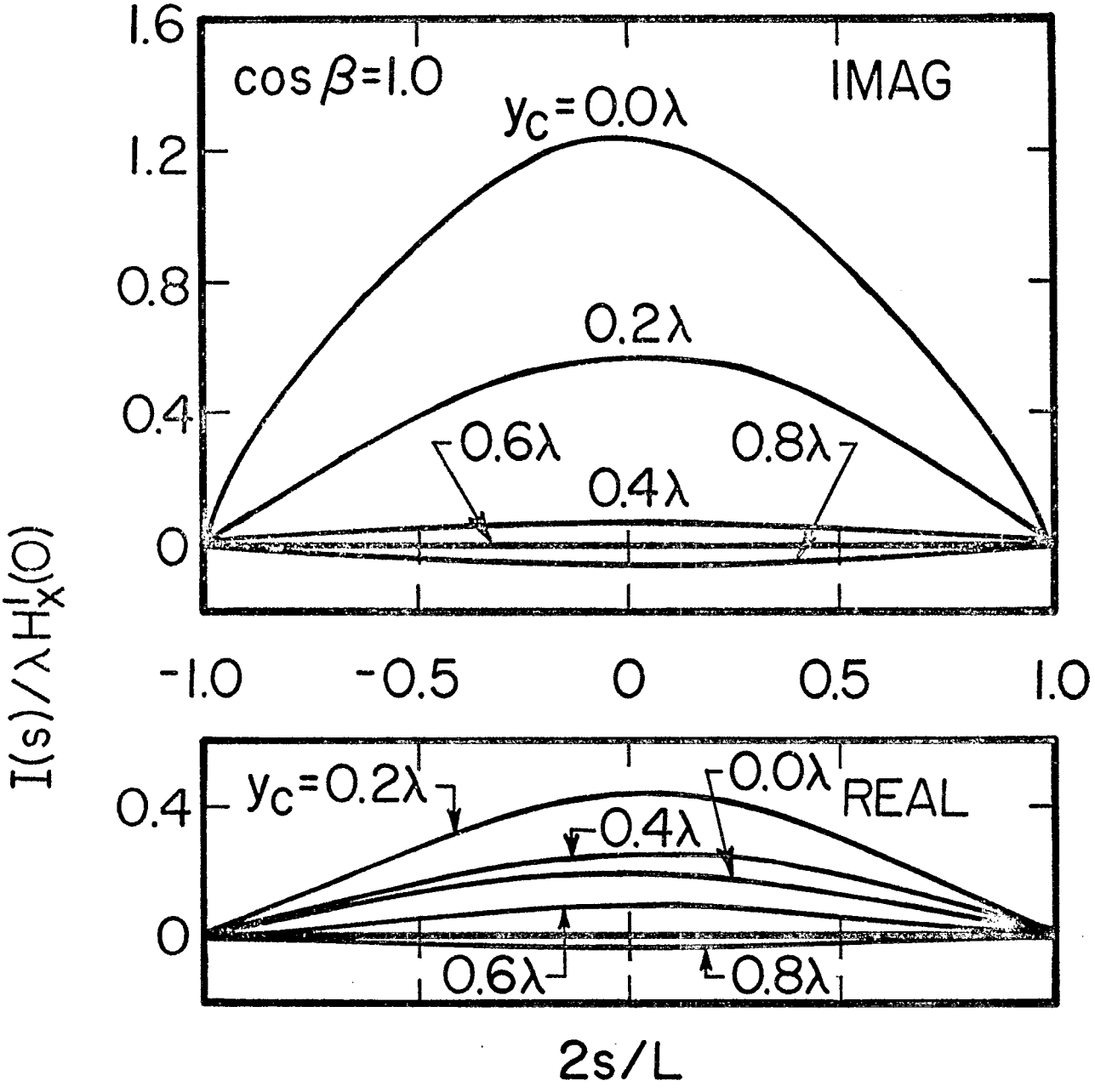

Fig. 8. Current on Wire Illuminated through Slotted Screen ($w/\lambda = 0.05$, $\ell/\lambda = 0.5$; $a/\lambda = 0.001$, $L/\lambda = 0.5$; $x_c/\lambda = 0$, $z_c/\lambda = 0.25$; normal incidence)

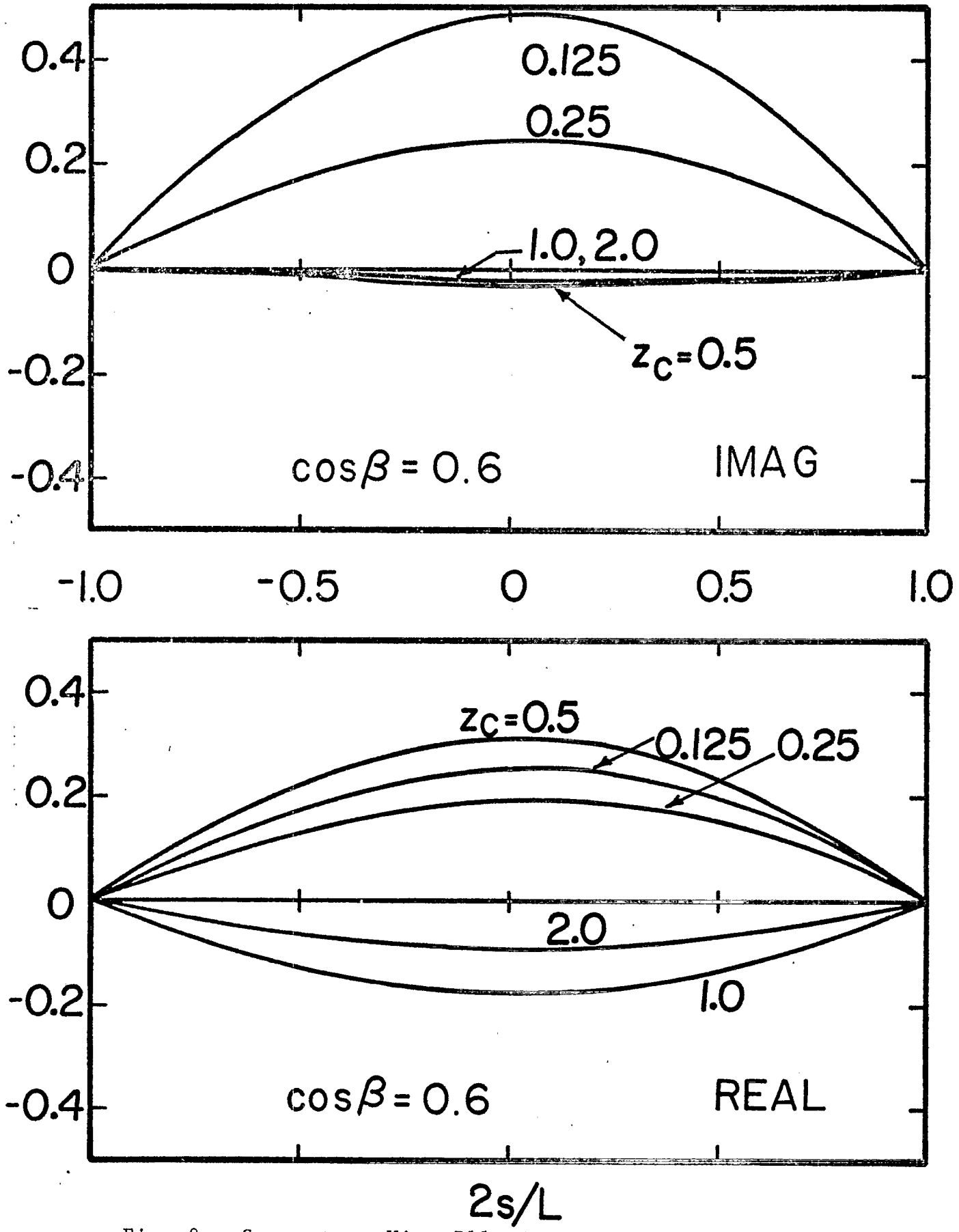

Fig. 9. Current on Wire Illuminated through Slotted Screen ($w/\lambda = 0.05$, $\ell/\lambda = 0.5$; $a/\lambda = 0.001$, $L/\lambda = 0.5$; $x_c/\lambda = 0.25$, $y_c/\lambda = 0$; normal incidence)

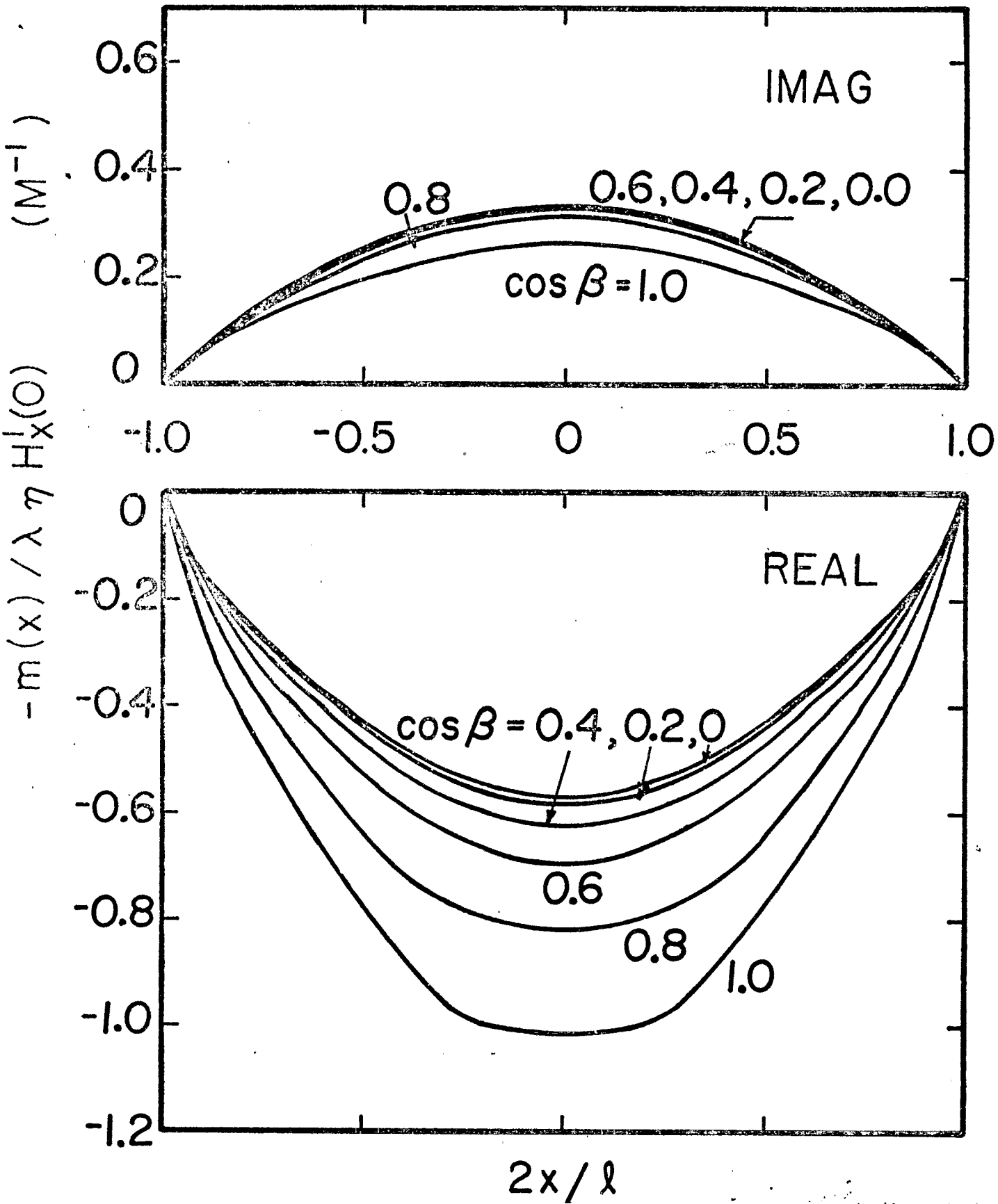

Fig. 10. Axial Distribution of Slot Magnetic Current ($w/\lambda = 0.05$, $\ell/\lambda = 0.5$; $a/\lambda = 0.001$, $L/\lambda = 0.5$; $x_c/\lambda = 0$, $y_c/\lambda = 0$, $z_c/\lambda = 0.25$; normal incidence)

Quarter-Wavelength Slot, Half-Wavelength Wire

Figs. 11-14 illustrate results for a quarter-wavelength slot and a half-wavelength wire. From these data we see, in general, that the shorter, quarter-wavelength slot passes less radiation than does the resonant, half-wavelength slot. Although a small degree of asymmetry is seen in Fig. 13, the current deviates only slightly from the resonant distribution. The scattering from the wire back into the quarter-wavelength slot is significant as seen in Fig. 14 but is not as significant as in the case of the half-wavelength slot (Fig. 10).

Half-Wavelength Slot, One-Wavelength Wire

In Figs. 15-20 are given data for the situation of a half-wavelength slot and a one-wavelength wire. The current displayed in Fig. 15 is on a wire whose center falls on the z axis (0,0, 0.125λ) so for any value of β the slot radiation gives rise to an even-function excitation of the wire which, in turn, causes an even-function current. If the wire center is displaced from the z axis along the slot axis to the point $(0.25\lambda,0,0.125\lambda)$, the current is seen in Fig. 16 to be quite different. Still, for $\cos\beta=1$, the excitation and, hence, the current are even, but, for any other value of $\cos\beta$, the excitation is not entirely an even function and, thus, the odd function antiresonant current is strongly excited on the one-wavelength wire. With the wire axis not above the slot axis, the wire excitation is never an even function and a strong antiresonant current is excited for all angles β (Figs. 17 and 18). The axial magnetic current m(x)

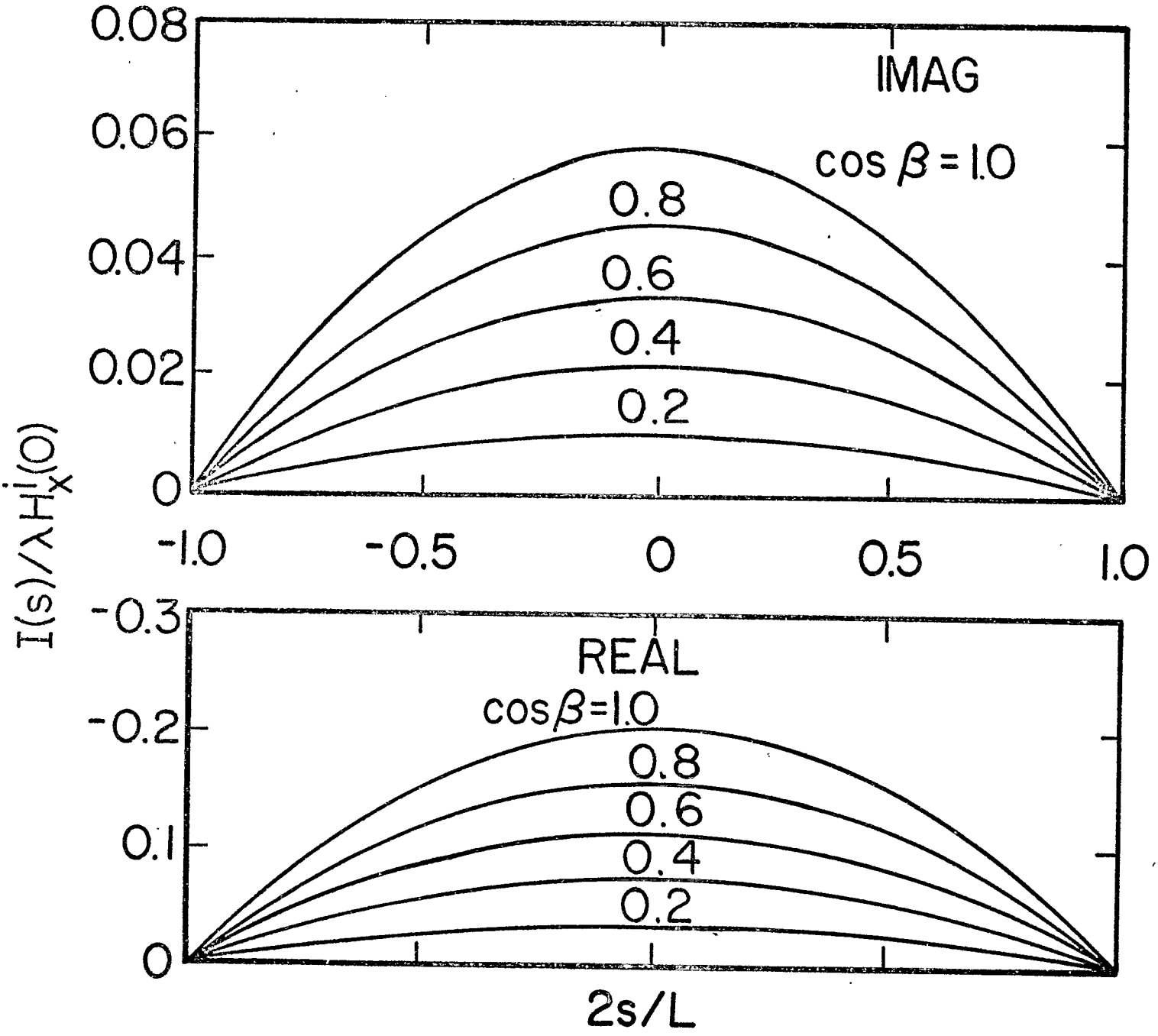

Fig. 11. Current on Wire Illuminated through Slotted Screen ($w/\lambda = 0.05$, $\ell/\lambda = 0.25$; $a/\lambda = 0.001$, $L/\lambda = 0.5$; $x_c/\lambda = 0$, $y_c/\lambda = 0$, $z_c/\lambda = 0.125$; normal incidence)

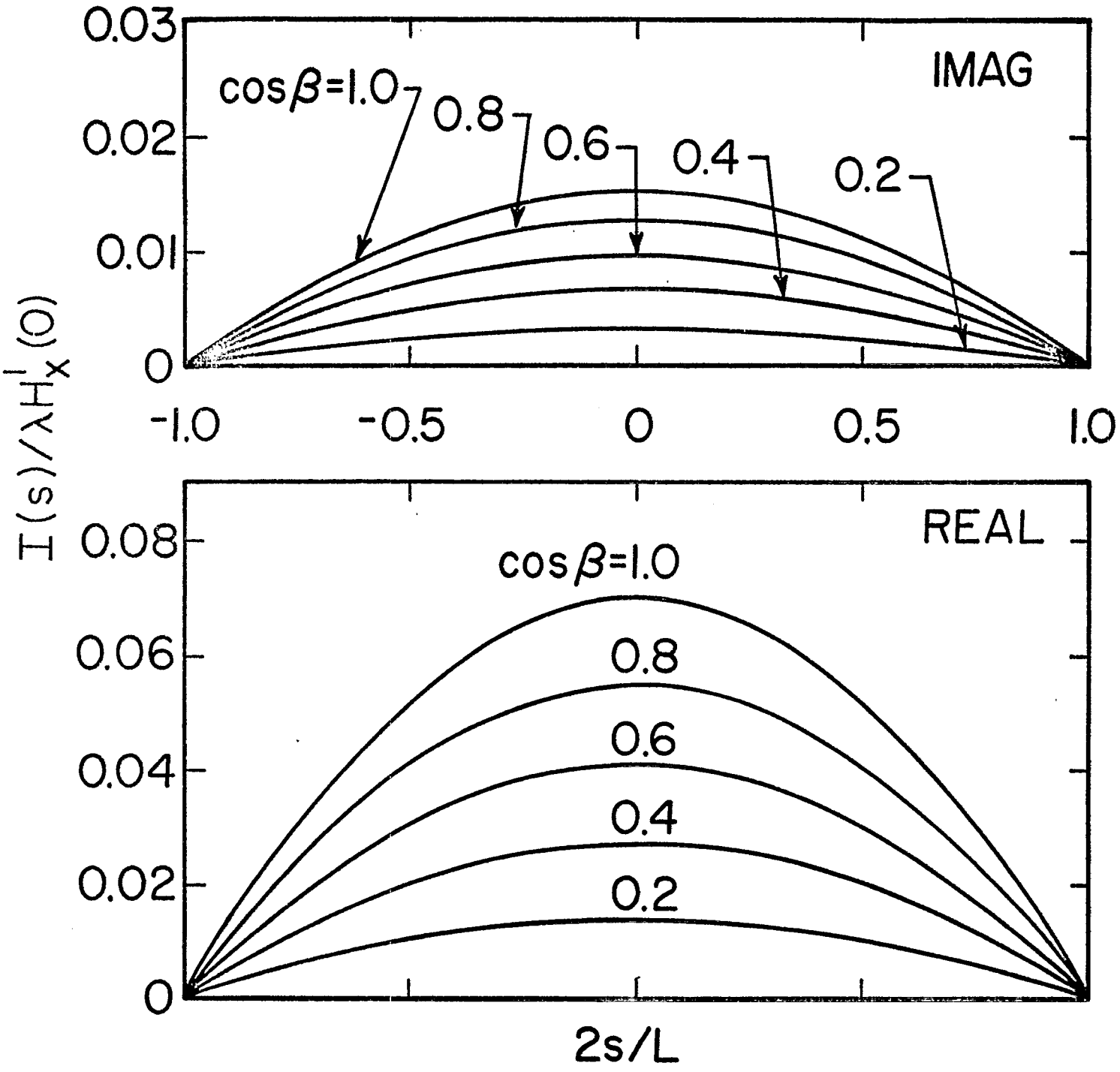

Fig. 12. Current on Wire Illuminated through Slotted Screen ($w/\lambda = 0.05$, $\ell/\lambda = 0.25$; $a/\lambda = 0.001$, $L/\lambda = 0.5$; $x_c/\lambda = 0$, $y_c/\lambda = 0$, $z_c/\lambda = 0.25$; normal incidence)

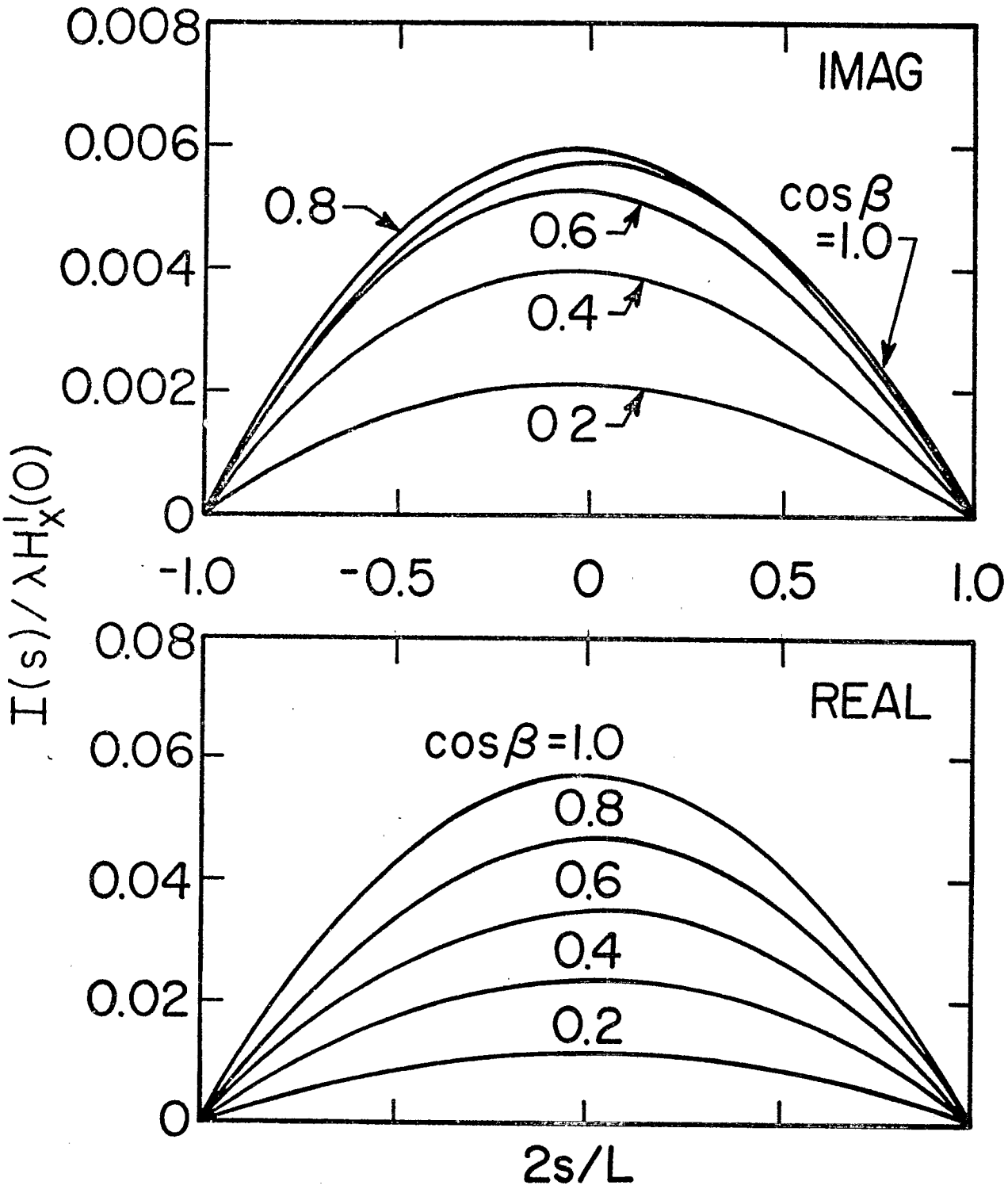

Fig. 13. Current on Wire Illuminated through Slotted Screen ($w/\lambda = 0.05$, $\ell/\lambda = 0.25$; $a/\lambda = 0.001$, $L/\lambda = 0.5$; $x_c/\lambda = 0.125$, $y_c/\lambda = 0$, $z_c/\lambda = 0.25$; normal incidence)

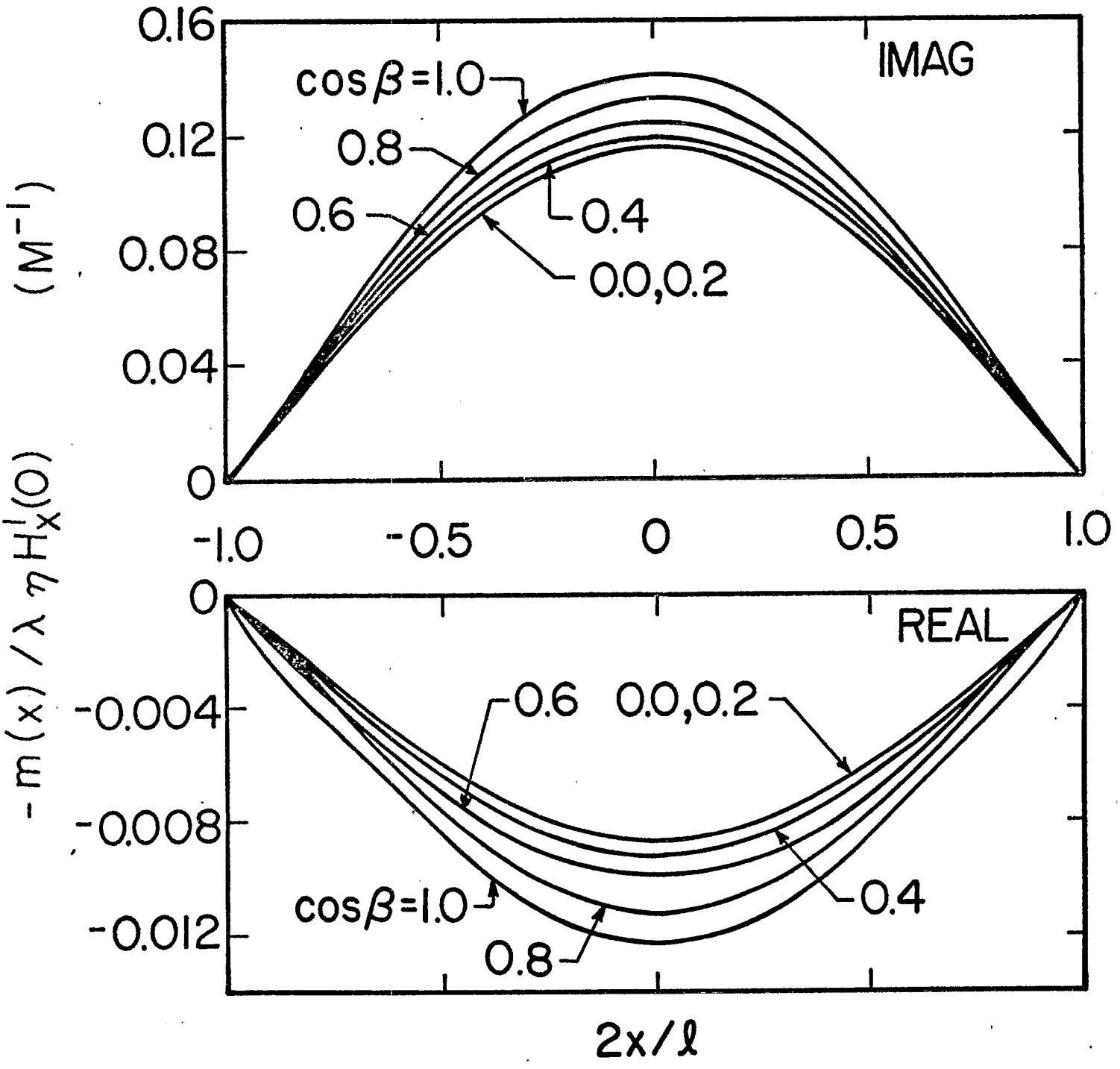

Fig. 14. Axial Distribution of Slot Magnetic Current ($w/\lambda = 0.05$, $\ell/\lambda = 0.25$; $a/\lambda = 0.001$, $L/\lambda = 0.5$; $x_c/\lambda = 0$, $y_c/\lambda = 0$, $z_c/\lambda = 0.125$; normal incidence)

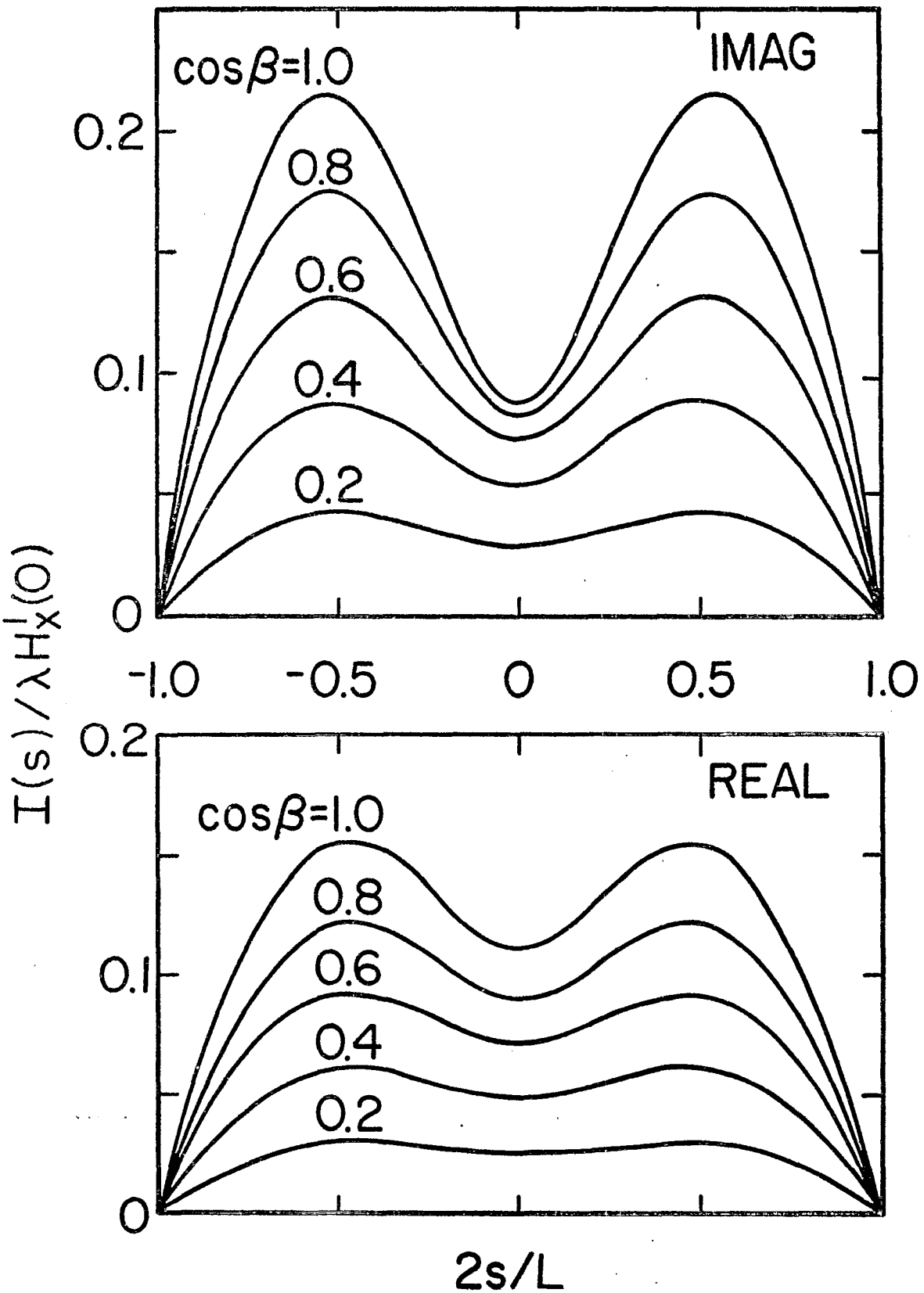

Fig. 15. Current on Wire Illuminated through Slotted Screen ($w/\lambda = 0.05$, $\ell/\lambda = 0.5$; $a/\lambda = 0.001$, $L/\lambda = 1.0$; $x_c/\lambda = 0$, $y_c/\lambda = 0$, $z_c/\lambda = 0.125$; normal incidence)

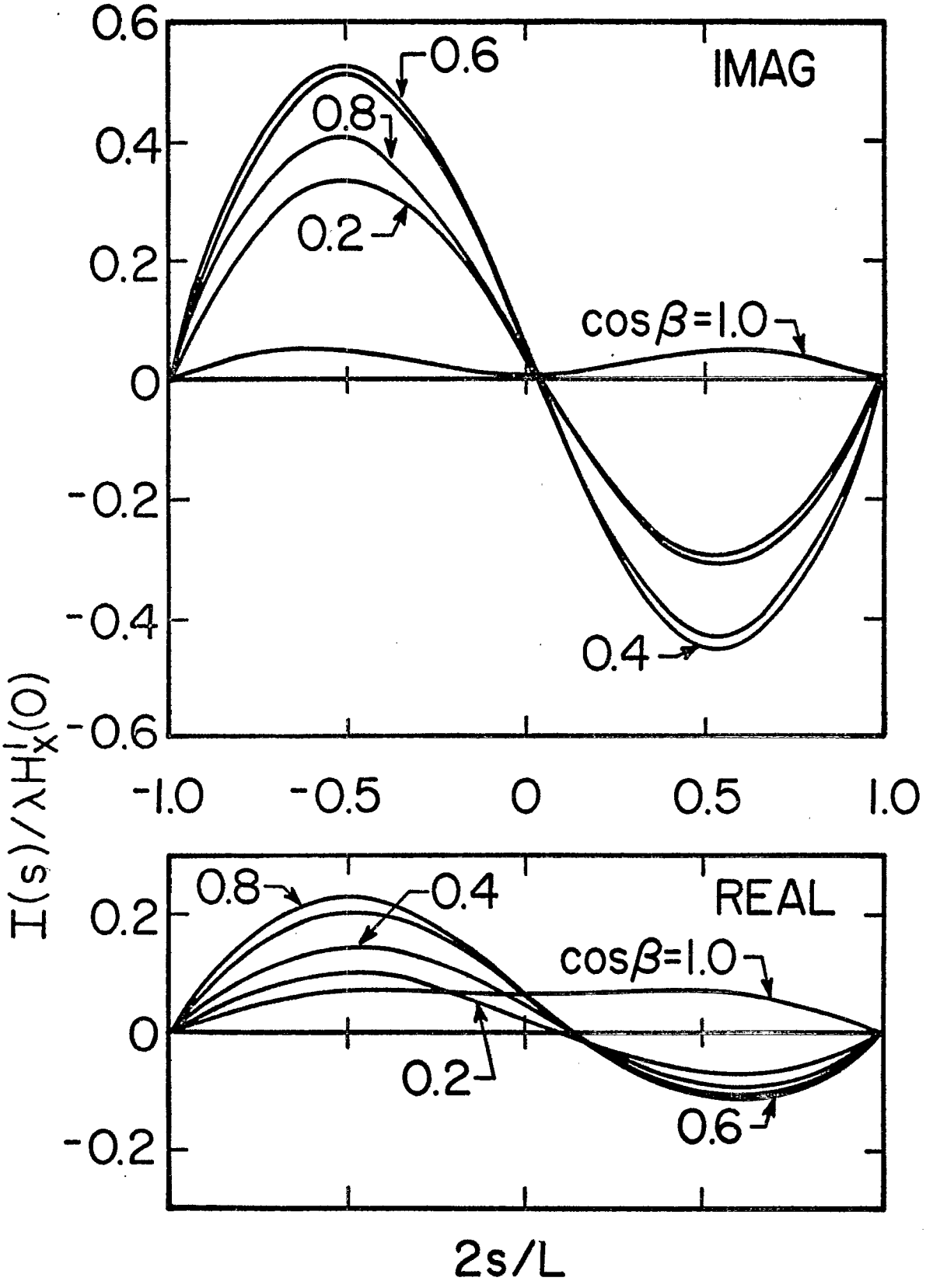

Fig. 16. Current on Wire Illuminated through Slotted Screen ($w/\lambda = 0.05$, $\ell/\lambda = 0.5$; $a/\lambda = 0.001$, $L/\lambda = 1.0$; $x_c/\lambda = 0.25$, $y_c/\lambda = 0$, $z_c/\lambda = 0.125$; normal incidence)

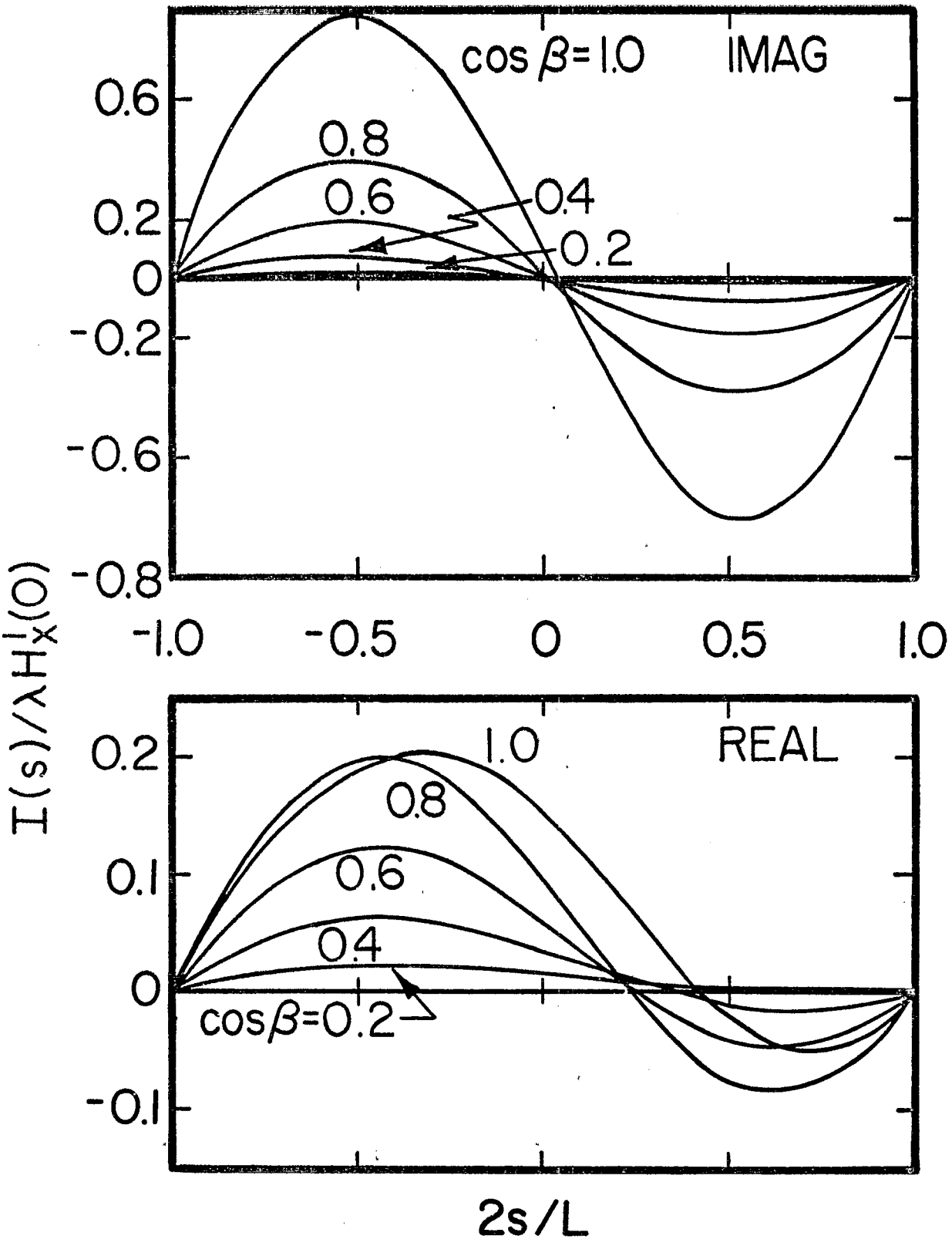

Fig. 17. Current on Wire Illuminated through Slotted Screen ($w/\lambda = 0.05$, $\ell/\lambda = 0.5$; $a/\lambda = 0.001$, $L/\lambda = 1.0$; $x_c/\lambda = 0$, $y_c/\lambda = 0.25$, $z_c/\lambda = 0.25$; normal incidence)

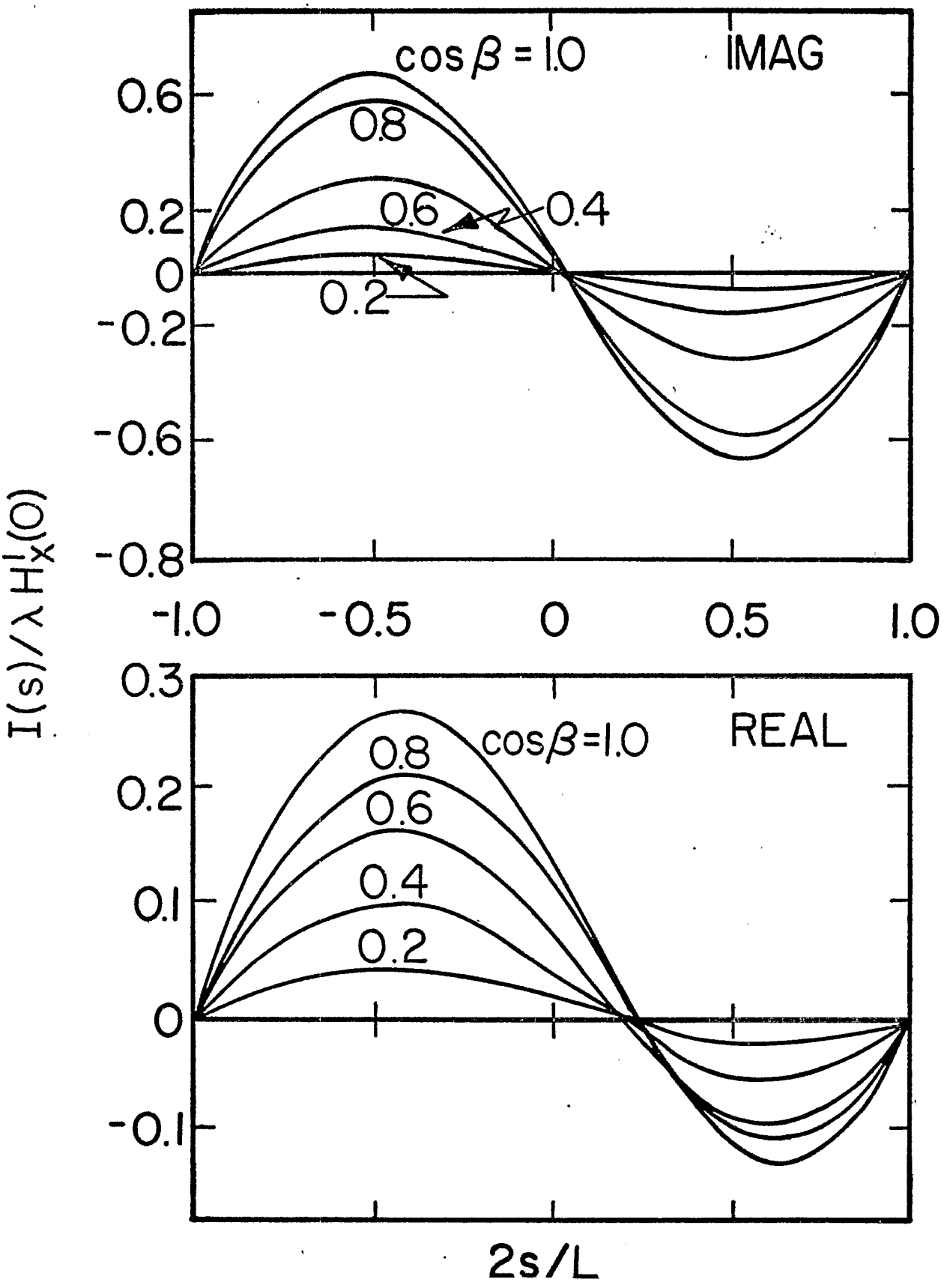

Fig. 18. Current on Wire Illuminated through Slotted Screen ($w/\lambda = 0.05$, $\ell/\lambda = 0.5$; $a/\lambda = 0.001$, $L/\lambda = 1.0$; $x_c/\lambda = 0.125$, $y_c/\lambda = 0.25$, $z_c/\lambda = 0.25$; normal incidence)

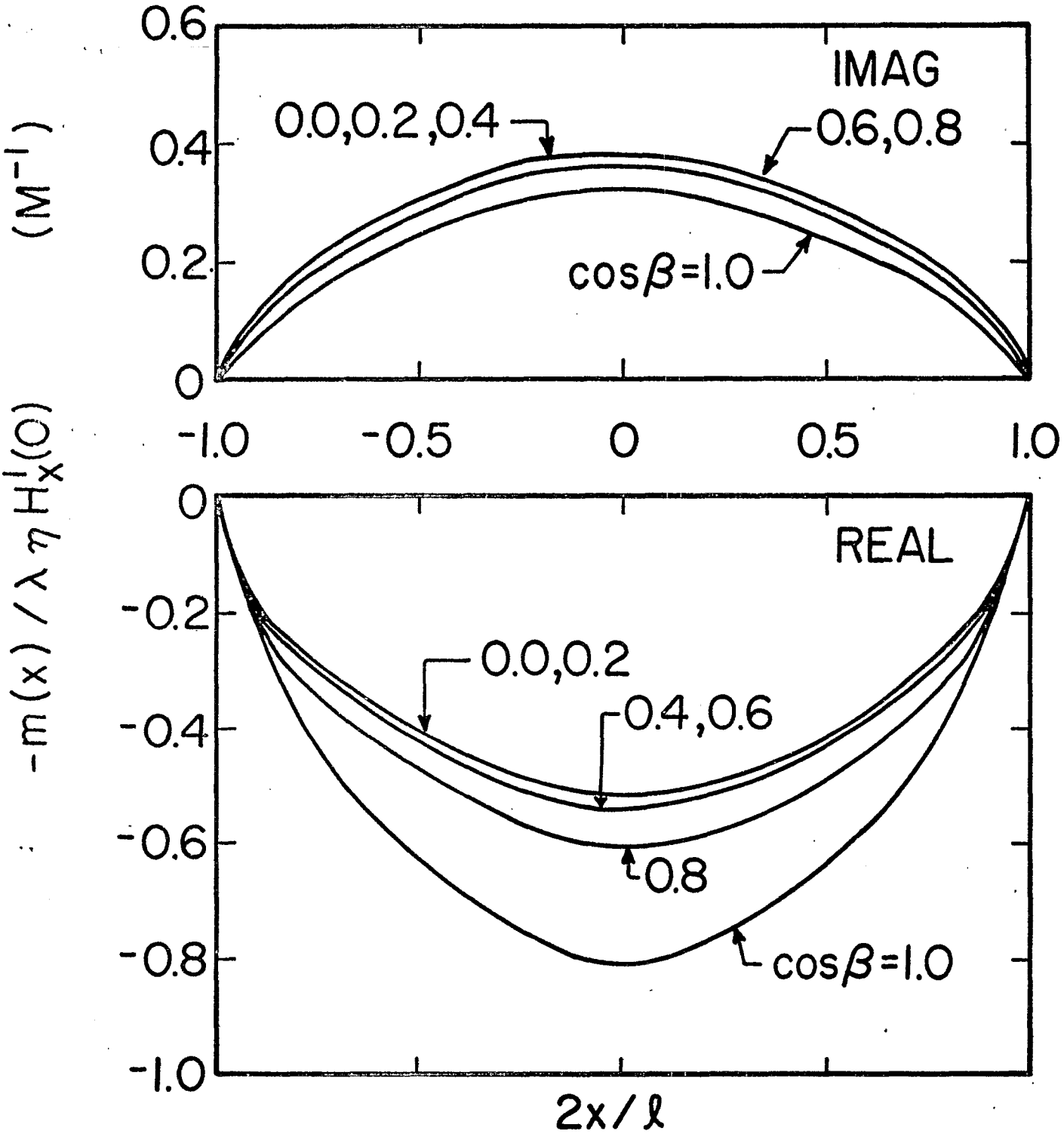

Fig. 19. Axial Distribution of Slot Magnetic Current ($w/\lambda = 0.05$, $\ell/\lambda = 0.5$; $a/\lambda = 0.001$, $L/\lambda = 1.0$; $x_c/\lambda = 0$, $y_c/\lambda = 0.25$, $z_c/\lambda = 0.25$; normal incidence)

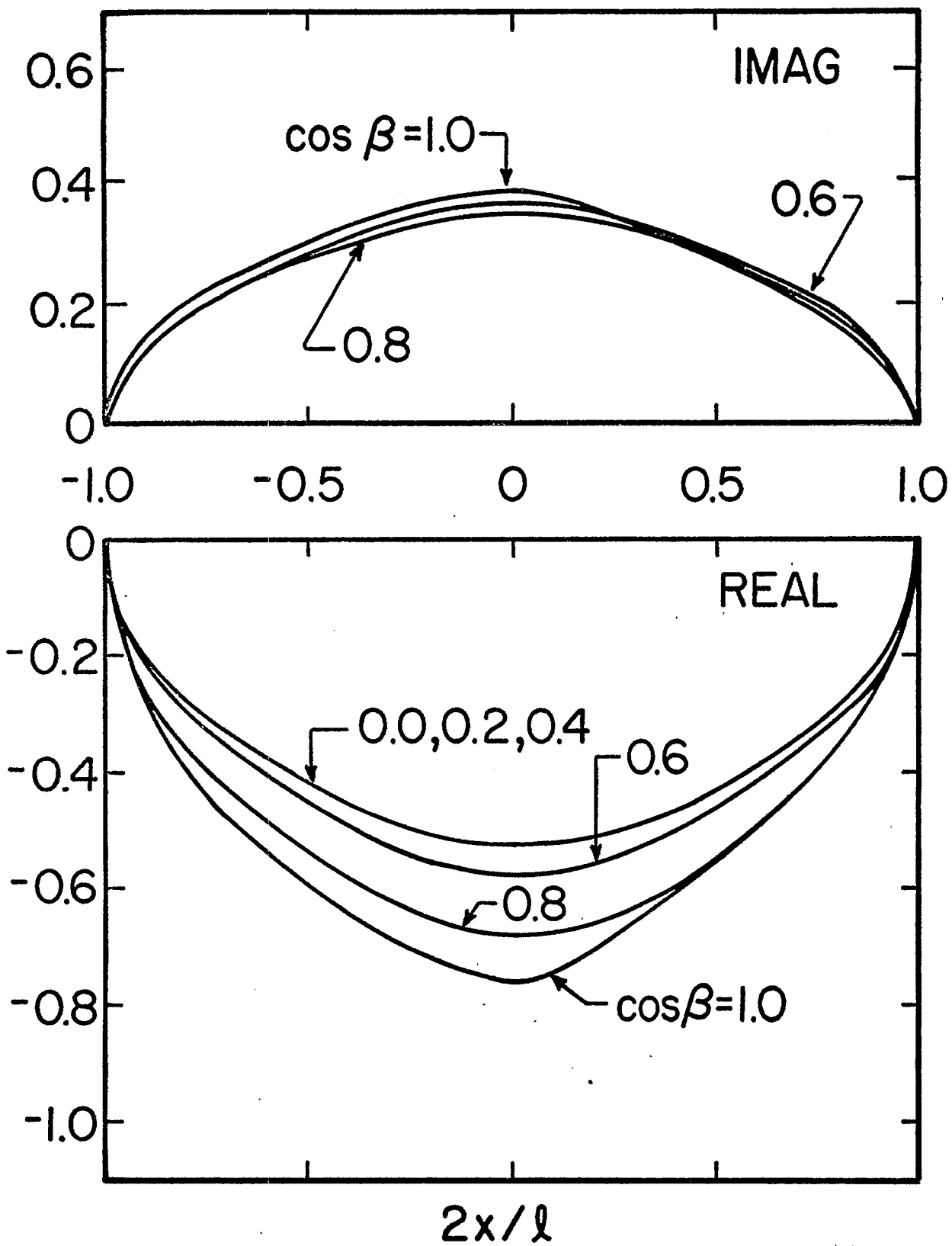

Fig. 20. Axial Distribution of Slot Magnetic Current ($w/\lambda = 0.05$, $\ell/\lambda = 0.5$; $a/\lambda = 0.001$, $L/\lambda = 1.0$; $x_c/\lambda = 0.125$, $y_c/\lambda = 0.25$, $z_c/\lambda = 0.25$; normal incidence)

in the half-wavelength slot (Fig. 19 and 20) is predominately resonant due to the plane wave excitation, which is normally incident and an even function, and the radiation scattered back from the wire has relatively little effect on this distribution. However, the coupling does influence the magnitude of the slot magnetic current.

One-Wavelength Slot, One-Wavelength Wire

Distributions of wire current and slot magnetic current are very sensitive to the location of the wire center and to β when the length of both the slot and the wire is one wavelength (Figs. 21-29). Figs. 21 and 22 depict current on a wire centered on the z axis at different distances behind the slotted screen. If the wire center is moved away from the z axis to a point still above the slot axis, again the one-wavelength antiresonant current is excited whenever $\cos\beta \neq 1$ (Figs. 23 and 24). The data of Fig. 25 are for the same case as are those of Fig. 22 and they depict the behavior of slot magnetic current.

Figs. 26 and 27 display slot magnetic current and pertain to the same wire/slot configurations as do Figs. 23 and 24 with the wire centers located at $(0.25\lambda, 0, 0.125\lambda)$ and $(0.25\lambda, 0, 0.25\lambda)$, respectively. The dominant illumination of the slot is the incident field with a smaller excitation caused by scattering from the wire. The normally incident illumination is an entirely even-function excitation of the slot and, thus, gives rise to a slot magnetic current having a shifted cosine (forced response) distribution and having no odd-function antiresonant component.

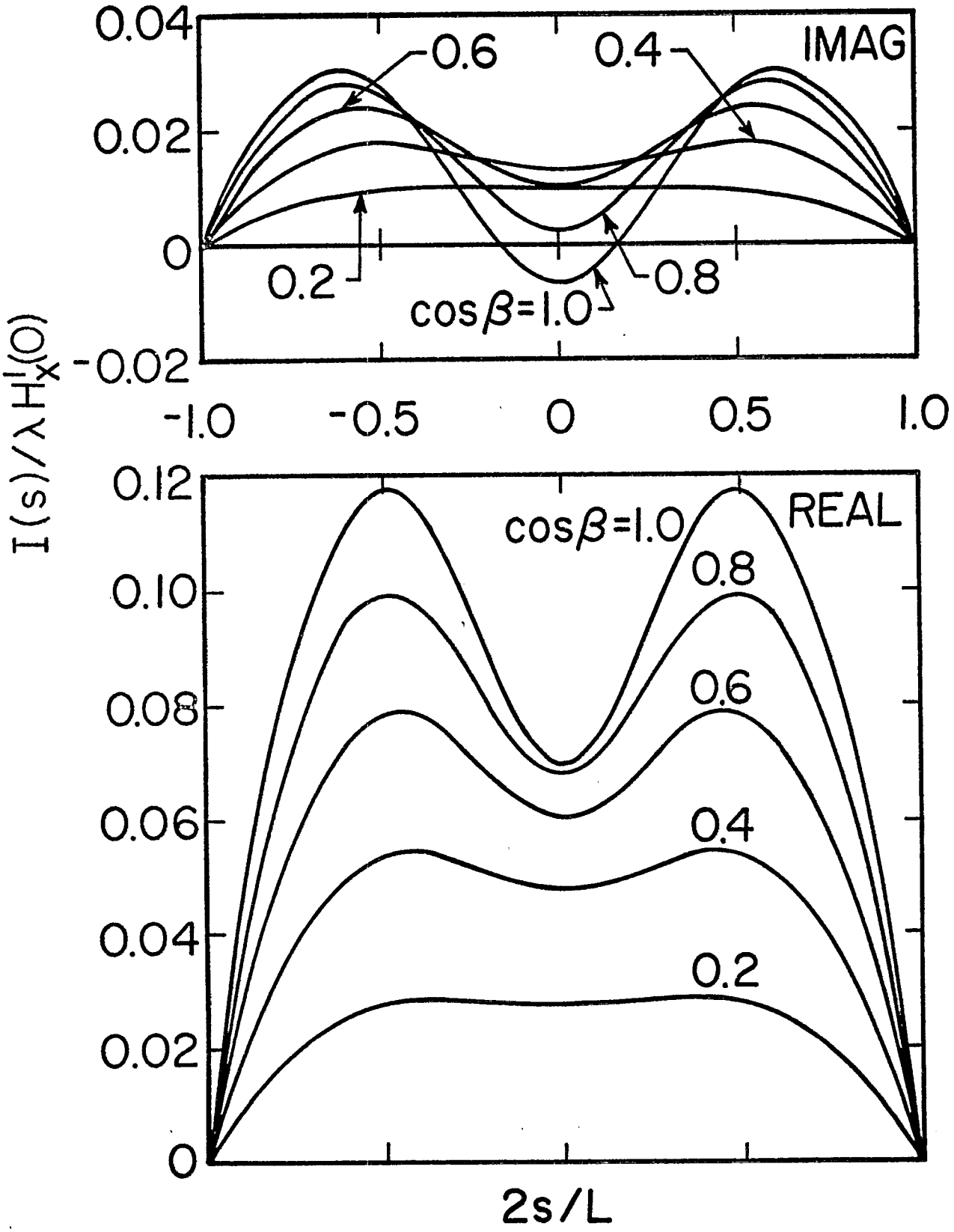

Fig. 21. Current on Wire Illuminated through Slotted Screen ($w/\lambda = 0.05$, $\ell/\lambda = 1.0$; $a/\lambda = 0.001$, $L/\lambda = 1.0$; $x_c/\lambda = 0$, $y_c/\lambda = 0$, $z_c/\lambda = 0.125$; normal incidence)

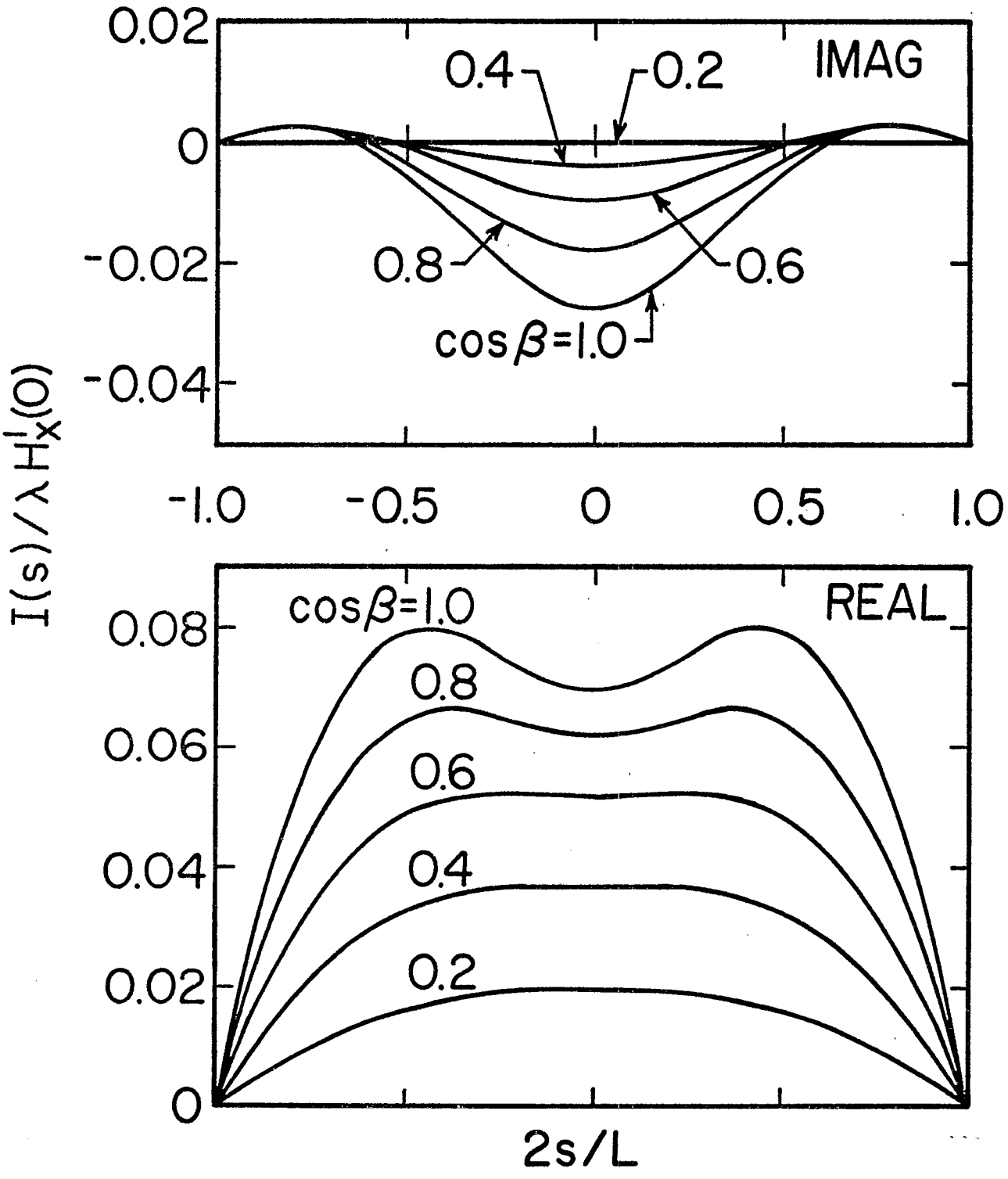

Fig. 22. Current on Wire Illuminated through Slotted Screen ($w/\lambda = 0.05$; $\ell/\lambda = 1.0$; $a/\lambda = 0.001$, $L/\lambda = 1.0$; $x_c/\lambda = 0$, $y_c/\lambda = 0$, $z_c/\lambda = 0.25$; normal incidence)

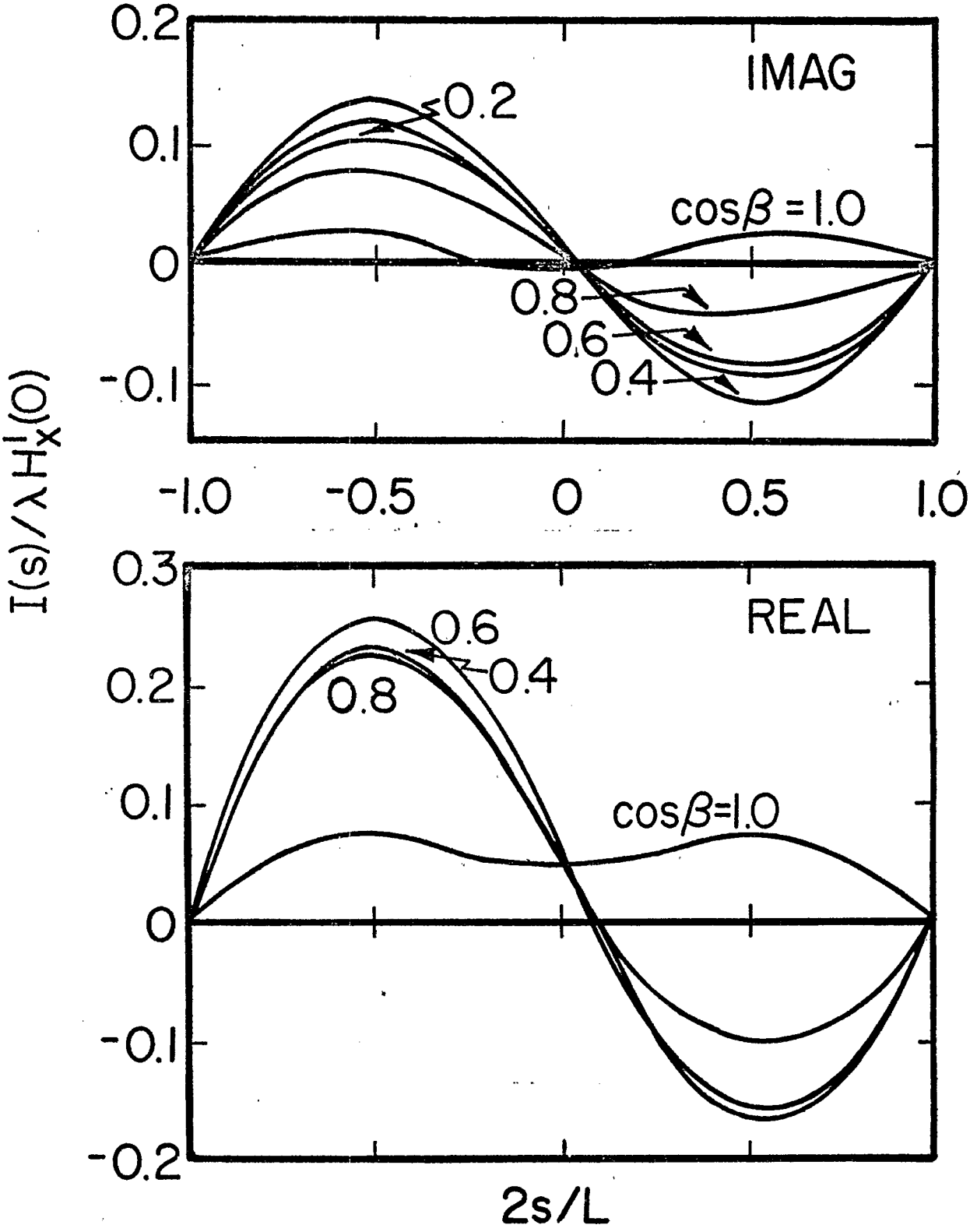

Fig. 23. Current on Wire Illuminated through Slotted Screen ($w/\lambda = 0.05$, $\ell/\lambda = 1.0$; $a/\lambda = 0.001$, $L/\lambda = 1.0$; $x_c/\lambda = 0.25$, $y_c/\lambda = 0$, $z_c/\lambda = 0.125$; normal incidence)

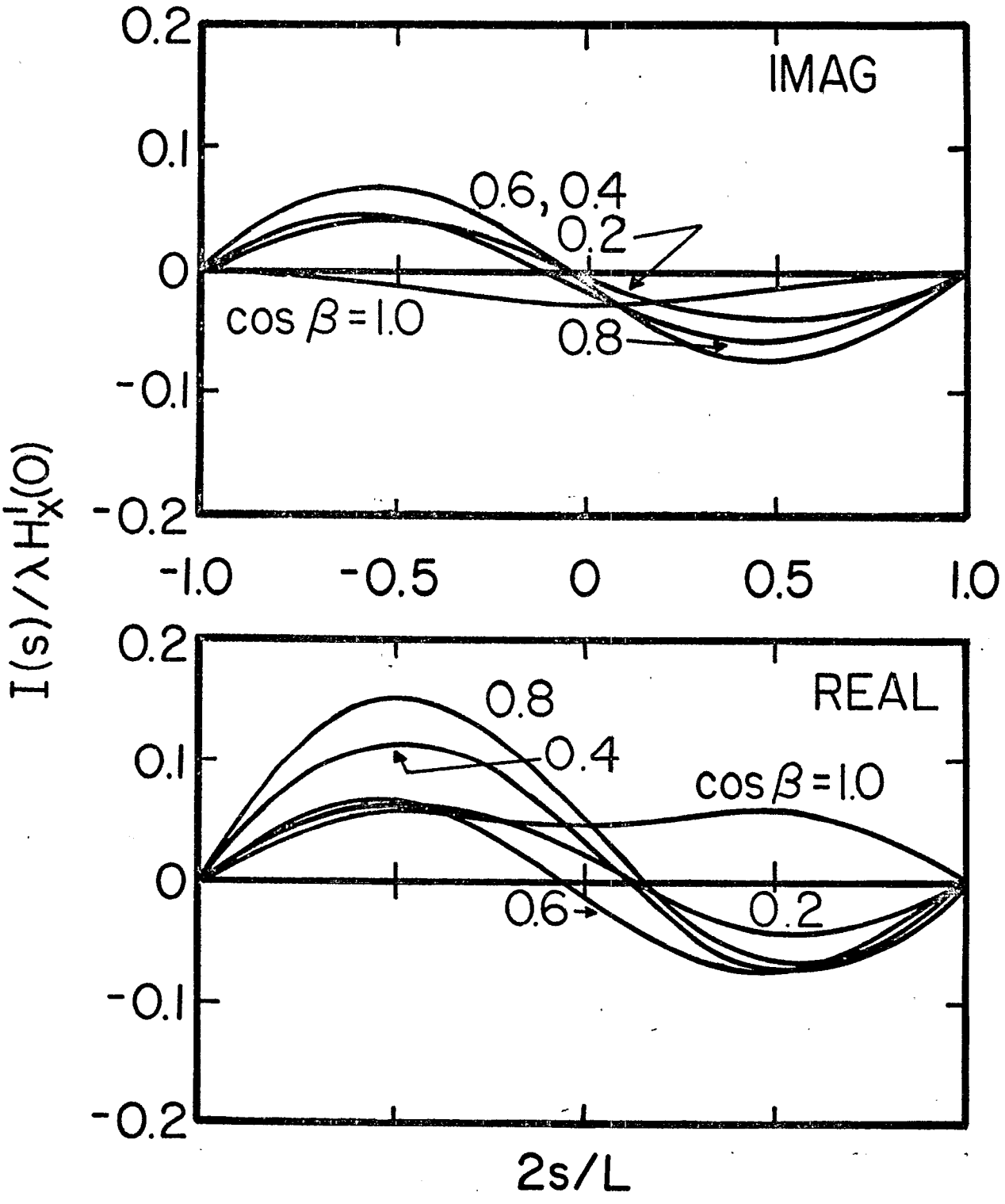

Fig. 24. Current on Wire Illuminated through Slotted Screen ($w/\lambda = 0.05$, $\ell/\lambda = 1.0$; $a/\lambda = 0.001$, $L/\lambda = 1.0$; $x_c/\lambda = 0.25$, $y_c/\lambda = 0$, $z_c/\lambda = 0.25$; normal incidence)

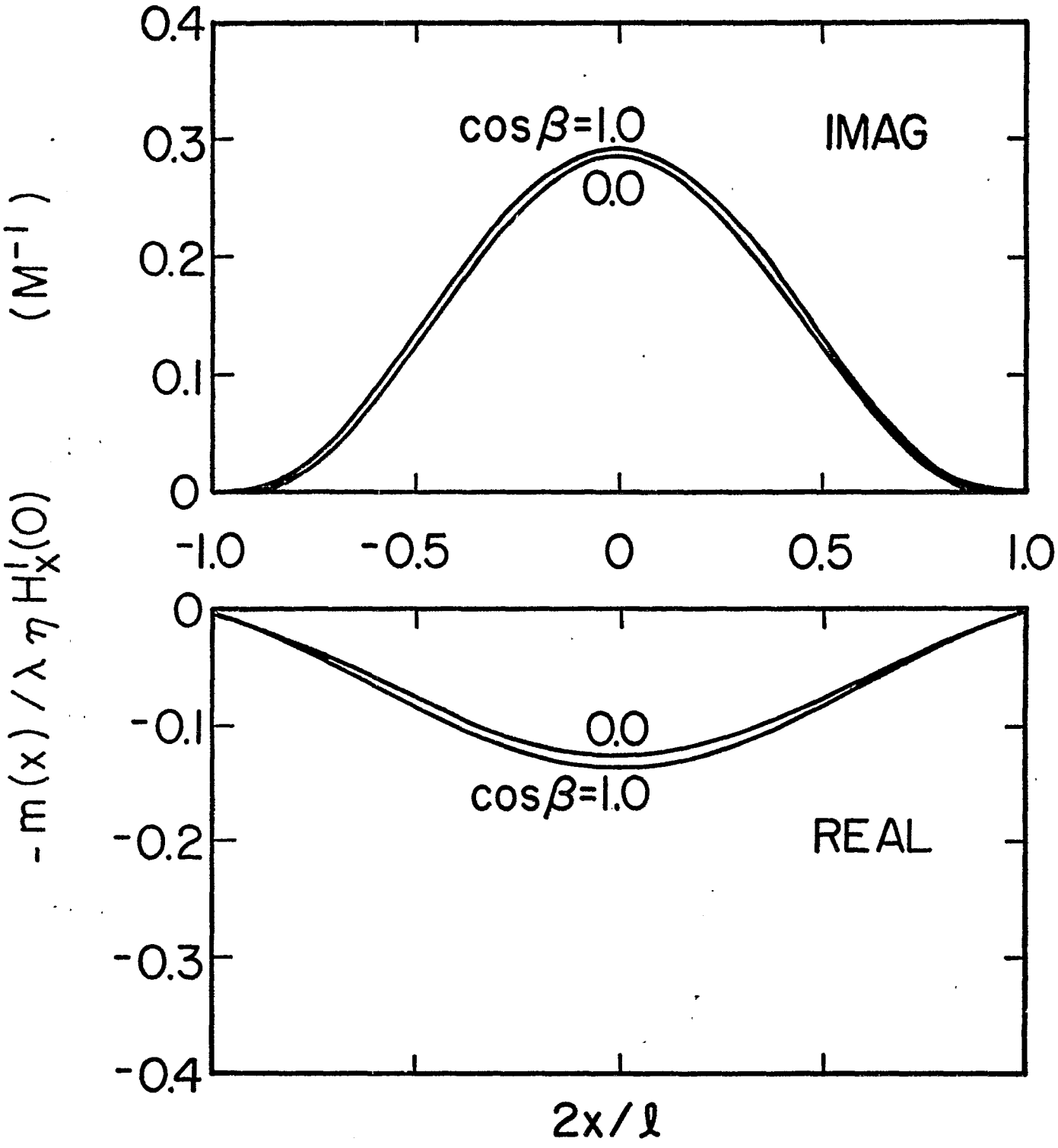

Fig. 25. Axial Distribution of Slot Magnetic Current ($w/\lambda = 0.05$, $\ell/\lambda = 1.0$; $a/\lambda = 0.001$, $L/\lambda = 1.0$; $x_c/\lambda = 0$, $y_c/\lambda = 0$, $z_c/\lambda = 0.25$; normal incidence)

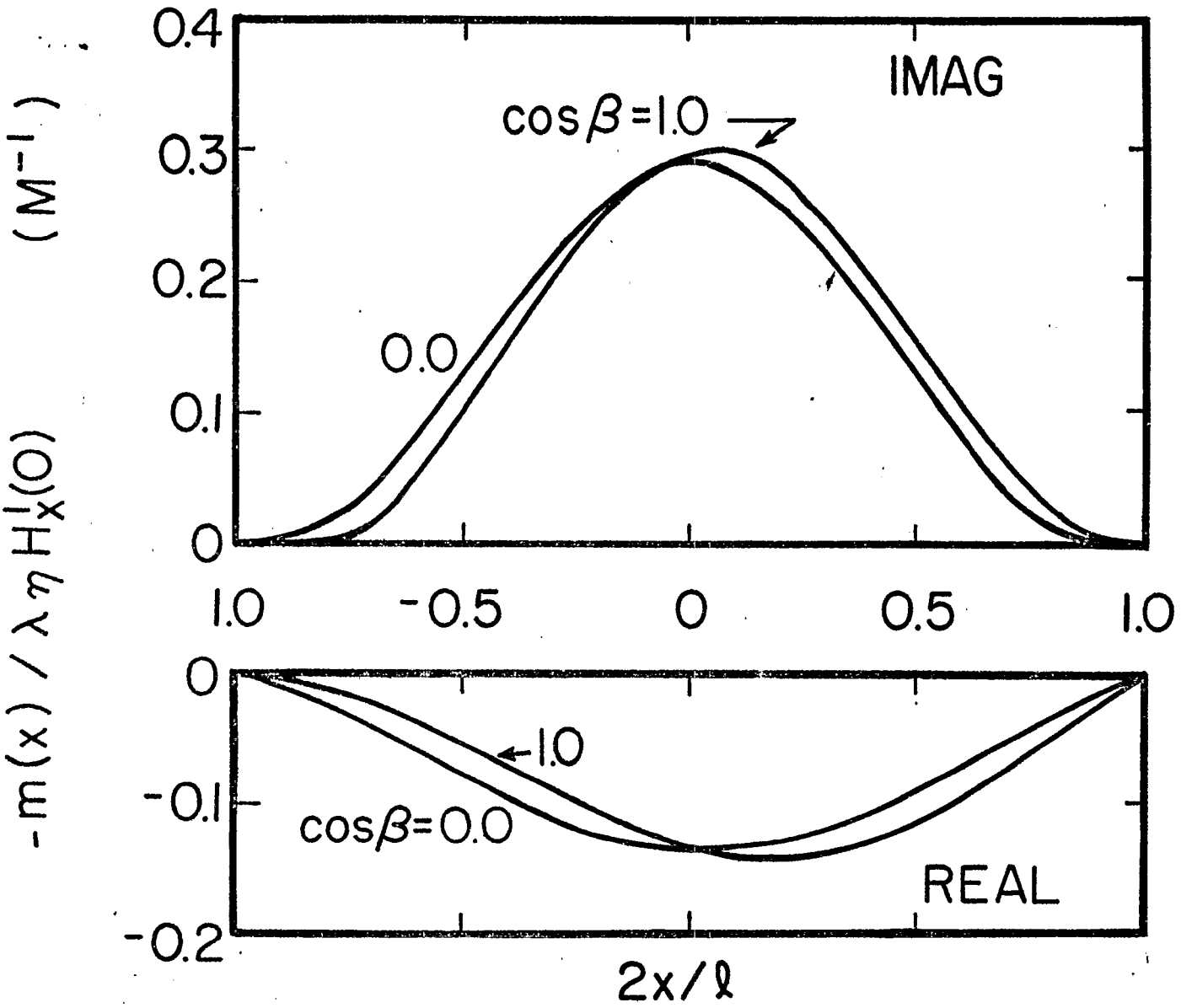

Fig. 26. Axial Distribution of Slot Magnetic Current ($w/\lambda = 0.05$, $\ell/\lambda = 1.0$; $a/\lambda = 0.001$, $L/\lambda = 1.0$; $x_c/\lambda = 0.25$, $y_c/\lambda = 0$, $z_c/\lambda = 0.125$; normal incidence)

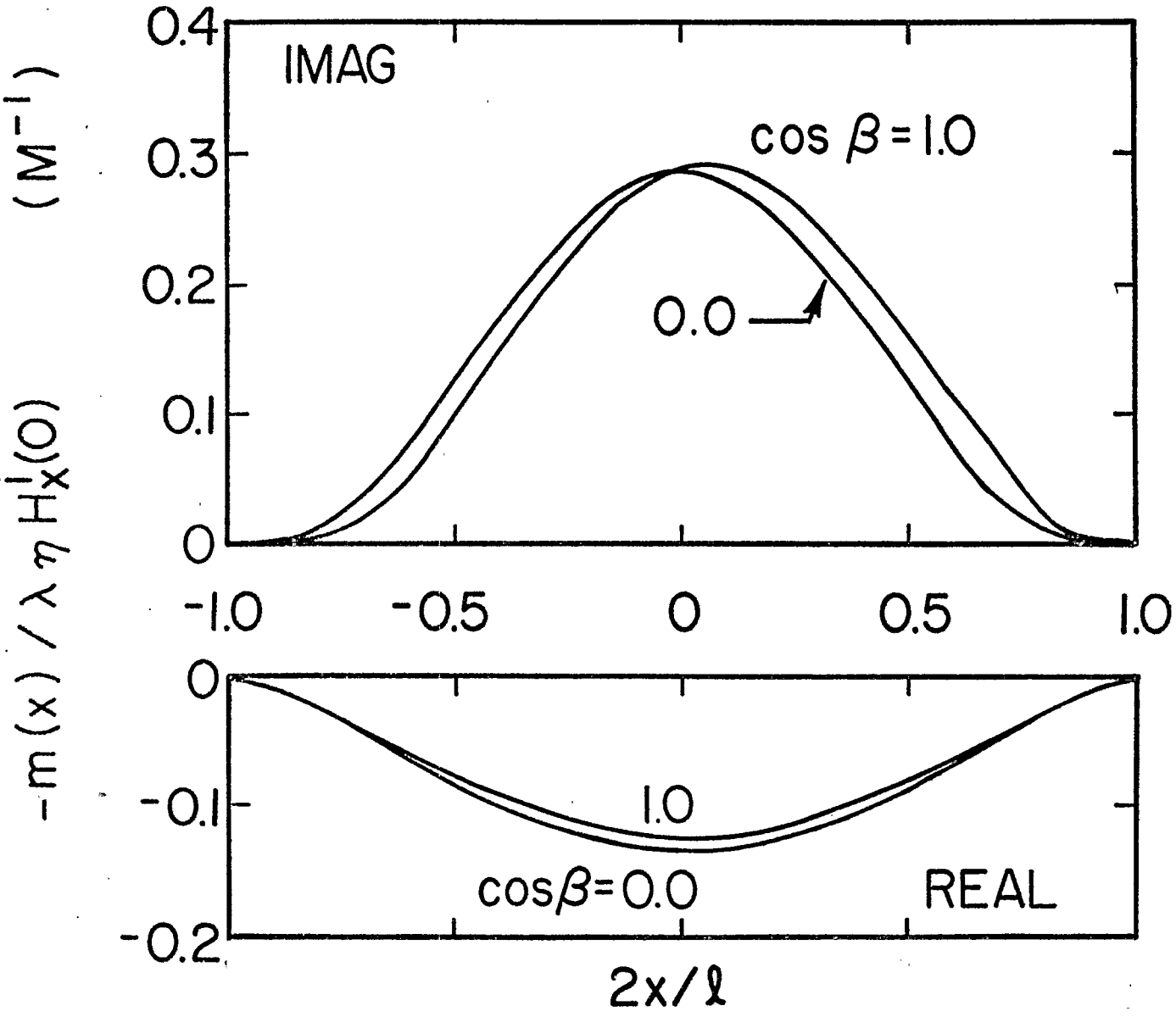

Fig. 27. Axial Distribution of Slot Magnetic Current ($w/\lambda = 0.05$, $\ell/\lambda = 1.0$; $a/\lambda = 0.001$, $L/\lambda = 1.0$; $x_c/\lambda = 0.25$, $y_c/\lambda = 0$ $z_c/\lambda = 0.25$; normal incidence)

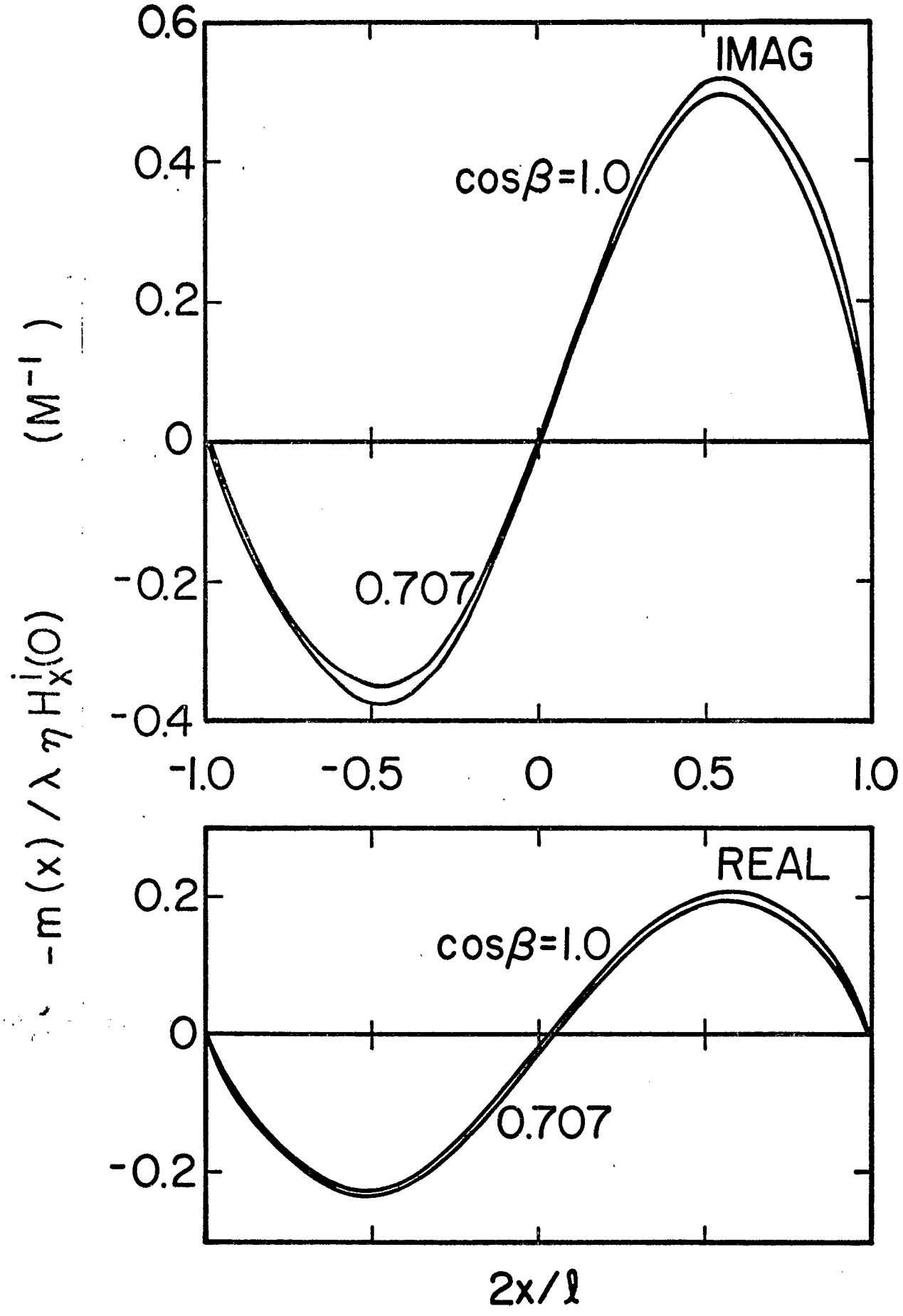

Fig. 28. Axial Distribution of Slot Magnetic Current ($w/\lambda = 0.05$, $\ell/\lambda = 1.0$, $a/\lambda = 0.001$, $L/\lambda = 1.0$; $x_c/\lambda = 0.25$, $y_c/\lambda = 0$, $z_c/\lambda = 0.25$; 60° - incidence angle)

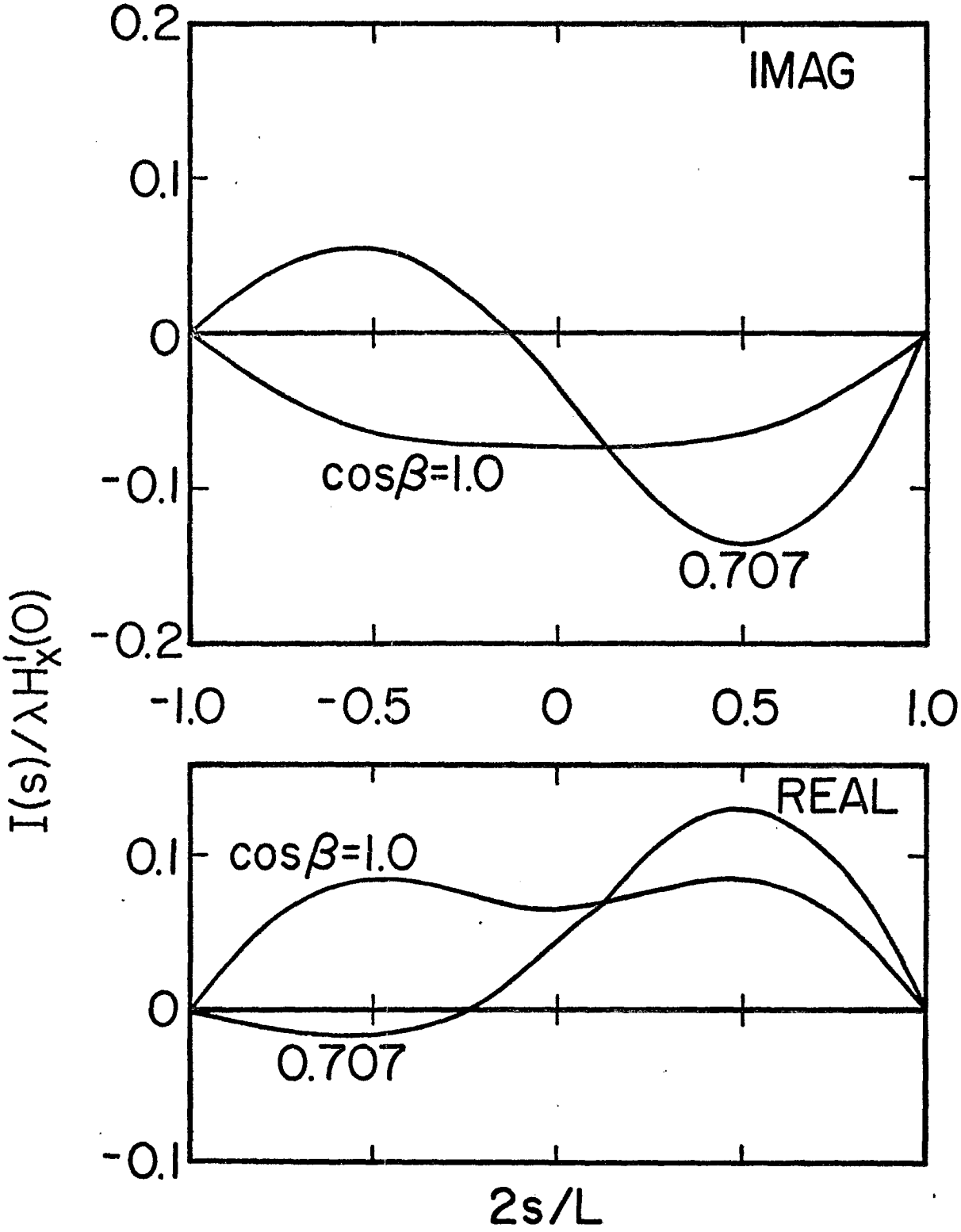

Fig. 29. Current on Wire Illuminated through Slotted Screen ($w/\lambda = 0.05$, $\ell/\lambda = 1.0$, $a/\lambda = 0.001$, $L/\lambda = 1.0$, $x_c/\lambda = 0.25$, $y_c/\lambda = 0$, $z_c/\lambda = 0.25$; 60^o - incidence angle)

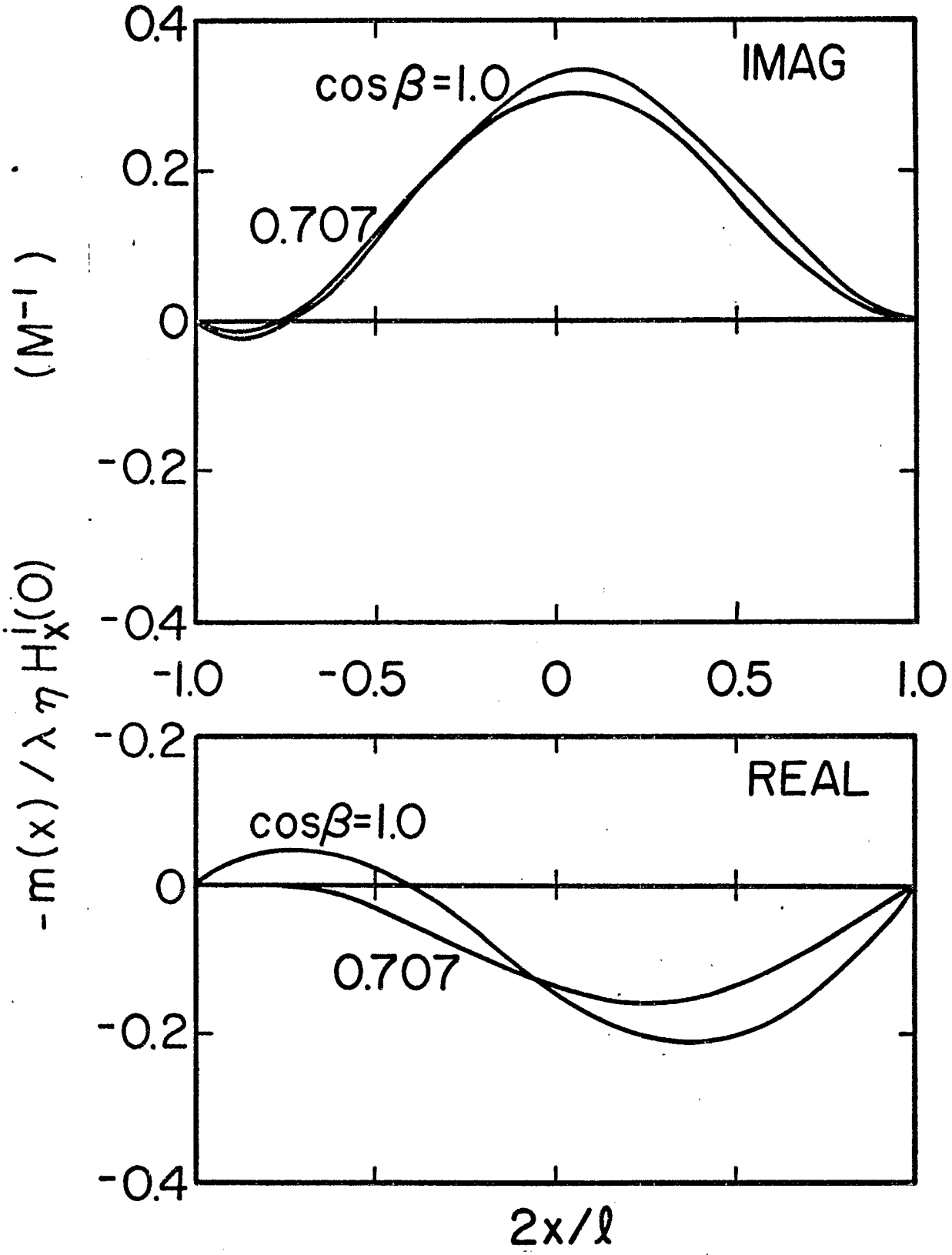

Fig. 30. Axial Distribution of Slot Magnetic Current ($w/\lambda = 0.05$, $\ell/\lambda = 1.0$, $a/\lambda = 0.001$, $L/\lambda = 0.5$; $x_c/\lambda = 0.25$, $y_c/\lambda = 0$, $z_c/\lambda = 0.25$; normal incidence)

For $\cos\beta=0$, there is, of course, no coupling between the wire and slot, so one observes in Figs. 26 and 27 the anticipated shifted cosine distribution, which is due only to the incident field forcing function. Even though the wire receives even-function excitation from the slot when $\cos\beta=1$ and the wire center is over the slot axis, the field scattered back from the wire to the slot does not represent an even excitation to the slot whenever the wire center is not on the z axis (regardless of the value of β). Thus, in Figs. 26 and 27 one observes for $\cos\beta=1$ the combination of a large forced magnetic current due to the incident field and a smaller antiresonant current due to the back scatter from the wire; the greater asymmetry observed in the curves of Fig. 26 compared to those of Fig. 27 is readily attributed to the differences in distance from the wire to the slotted screen in the two cases.

All results discussed above pertain to cases where the plane wave illumination is normally incident upon the slotted screen. An antiresonant magnetic current can be excited in a one-wavelength slot by an obliquely incident plane wave, and Figs. 28 and 29 display slot magnetic current and wire current under such conditions of illumination in which the angle between the z axis and the direction of propagation is 60°. The slot magnetic current

is seen in Fig. 28 to be strongly antiresonant, while the wire current in Fig. 29 contains an antiresonant component only when $\cos\beta \neq 1$ with the wire center at $(0.25\lambda, 0, 0.25\lambda)$. Such is exactly what one anticipates, since with the center of the wire above the slot axis and with $\cos\beta = 1$, the wire excitation is an even function independent of the slot magnetic current distribution. To assess the influence of the angle of incidence of the plane wave incident field, one should compare the curves of Figs. 28 and 29 to those of Figs. 27 and 24.

One-Wavelength Slot, Half-Wavelength Wire

As a final facet in the characterization of the present problem, we turn to Figs. 30 and 31 which show that, even with normally incident illumination, the non even-function excitation of the slot from the large resonant current on the half-wavelength wire is sufficiently large to cause significant antiresonant magnetic current in the one-wavelength slot to the extent that the resulting asymmetry in the distribution is quite noticeable. One should compare the data of Figs. 30 and 31 to those of Figs. 27 and 24 and observe the greater asymmetry in the curves of Fig. 30 than in those of Fig. 27. The larger asymmetry is due, primarily, to the greater current in the half-wavelength wire (Fig. 31) than that in the one-wavelength wire (Fig. 24) and, secondarily, to the fact that the current is maximum in the center of the half-wavelength wire nearest to the slot while the current in the one-wavelength wire is minimum at its center.

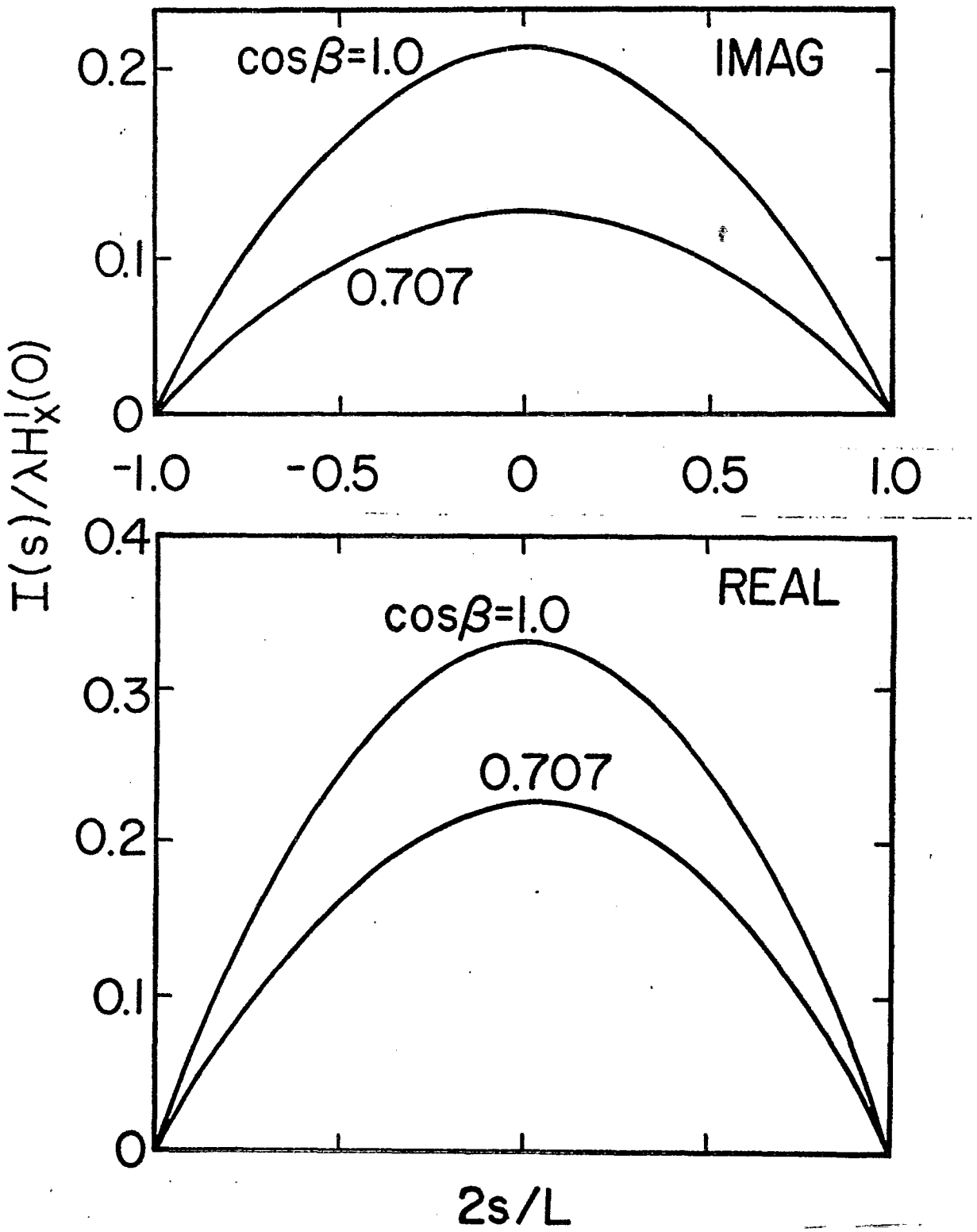

Fig. 31. Current on Wire Illuminated through Slotted Screen ($w/\lambda = 0.05$, $\ell/\lambda = 1.0$; $a/\lambda = 0.001$, $L/\lambda = 0.5$; $x_c/\lambda = 0.25$, $y_c/\lambda = 0$, $z_c/\lambda = 0.25$; normal incidence)

REFERENCES

1. King, R. W. P., G. H. Owyang, "The Slot Antenna with Coupled Dipoles," IRE Trans. on Antennas and Propagation, Vol. AP-8, No. 2, pp. 136-143; March, 1960.

2. Lin, J. L., Curtis, W. L., and M. C. Vincent, "Electromagnetic Coupling to a Cable through Apertures," 1974 International IEEE/AP-S Symposium Digest, Atlanta, Georgia, pp. 196-199; June, 1974.

3. Butler, C. M., "Analysis of a Wire Excited through an Aperture Perforated Conducting Screen," 1974 URSI Annual Meeting, Boulder, Colorado; October, 1974.

4. Rahmat-Samii, Y., and R. Mittra, "Integral Equation Solution and RCS Computation of a Thin Rectangular Plate," Interaction Note 156, December 1973.

5. Lin, J. L., Curtis, W. L., and M. C. Vincent, "On the Field Distribution of an Aperture," IEEE Trans. on Antennas and Propagation, Vol. Ap-22, No. 3, pp. 467-471; May, 1974.

6. King, R. W. P., The Theory of Linear Antennas, Harvard University Press, Cambridge, Massachusetts; 1956.

7. Harrington, R. F., Field Computation by Moment Methods, MacMillan, New York; 1968.